To date, however, distinct molecular markers on CSCs are still lacking in many cancers. Moreover, only a few reports have shown the existence of CSCs in bone and soft tissue sarcomas (Gibbs *et al*, 2005; Wu *et al*, 2007; Tirino *et al*, 2008). In this study, with the goal of determining specific markers of CSCs, we identified and characterised SP cells having cancer-initiating ability in osteosarcoma and bone malignant fibrous histiocytoma cell lines.

MATERIALS AND METHODS

Cell lines and culture

Seven human osteosarcoma (OS) cell lines (OS2000, KIKU, NY, Huo9, HOS, U-2OS and Saos2) and one bone human malignant fibrous histiocytoma (MFH) cell line (MFH2003) were used. OS2000, KIKU and MFH2003 were established in our laboratory (Wada *et al*, 1988; Nabeta *et al*, 2003; Tsukahara *et al*, 2006). The other cell lines were kindly donated by or purchased from the Japanese Collection of Research Bioresources Cell Bank (Tokyo, Japan) and from the American Type Culture Collection (Manassas, VA, USA). MFH2003 and OS2000 were cultured with Iscove's modified Dulbecco's Eagle's medium (IMDM; GIBCO BRL, Grand Island, NY, USA) containing 10% FBS and the others were maintained in Dulbecco's modified Eagle's medium (DMEM; Sigma-Aldrich, St Louis, MO, USA) containing 10% FBS in a 5% CO_2 incubator at 37°C.

Identification of side population

Cell suspensions were labelled with dye Hoechst 33342 (Cambrex Bio Science Walkersville Inc., MD, USA) using the methods described by Goodell *et al* (1996) with some modifications . Briefly, cells were trypsinised and re-suspended in pre-warmed DMEM supplemented with 5% FBS at a concentration of $1 \times 10^6\,ml^{-1}$. Hoechst33342 dye was added at a final concentration of 2.5 or $5.0\,\mu g\,ml^{-1}$ in the presence or absence of verapamil (50 or 75 μM; Sigma-Aldrich) as an inhibitor of the ABC transporter. The cells were incubated at 37°C for 90 min with continuous shaking. At the end of the incubation, the cells were washed with ice-cold PBS with 5% FBS, centrifuged at 4°C and resuspended in ice-cold PBS containing 5% FBS. Propidium iodide (at a final concentration of $1\,\mu g\,ml^{-1}$; Molecular Probes–Invitrogen, Eugene, OR, USA) was used to gate viable cells. Flow cytometry and cell sorting were performed using FACSVantage SE (BD Biosciences, Bedford, MA, USA), EPICS ALTRA (Beckman-Coulter, Fullerton, CA, USA) and FACS Aria II (BD Biosciences). The Hoechst 33342 dye was excited at 357 nm and its fluorescence was analysed using dual wavelengths (blue, 402–446 nm; red, 650–670 nm).

RNA preparation

Total RNAs were extracted from SP cells and MP cells using the RNeasy Mini kit (Qiagen, Hilden, Germany) according to the manufacturer's protocol. Using an Amino Allyl MessageAmp aRNA Kit Ver. 2 (Sigma-Aldrich Japan, Ishikari, Japan), amino allyl-modified aRNAs were prepared from total RNAs from SP and MP cells as previously described (Takeuchi *et al*, 2008).

Real-time PCR analysis

Total RNA was reverse transcribed using the SuperScriptIII reverse transcriptase enzyme (Invitrogen) according to the manufacturer's instructions. Real-time PCR was performed with SYBR Green Real-time Core Reagent (Applied Biosystems, Foster City, CA, USA) according to the manufacturer's instructions on an ABI Prism 7900 Sequence Detection System (Applied Biosystems). Primers were designed to generate a PCR product of <200 bp. The thermal cycling conditions were 94°C for 2 min, followed by 35 cycles of 15 s at 94°C, 30 s at 60°C and 30 s at 72°C. Levels of expression were normalised to the *glyceraldehyde-3-phosphate dehydrogenase* (G3PDH) housekeeping gene.

Spherical colony formation assay

Spherical colony formation assay was performed as described by Gibbs *et al* (2005) with some modifications. Briefly, cells were plated at 2000 cells per well in six-well ultra-low attachment plates (Corning Inc., Corning, NY, USA). Mesenchymal Stem Cell Basal Medium (MSCBM) and MSCBM SingleQuots (Takara Bio Inc., Ohtsu, Japan) were used for cell culture. Fresh aliquots of epidermal growth factor and basic fibroblast growth factor were added every other day. On day 14, the numbers of colonies were counted.

Xenograft model

Sorted SP and MP cells of MFH2003 were collected and re-suspended at $1 \times 10^2 - 1 \times 10^5$ cells per 50 μl of PBS, followed by addition of 50 μl of Matrigel (BD Biosciences). This cell-Matrigel suspension was subcutaneously injected into the backs of 4- to 6-week-old non-obese diabetic/severe combined immunodeficiency (NOD/SCID) mice (NOD.CB17-Prdkc^{scid}/J, Charles River Laboratory, Yokohama, Japan) under anaesthesia. Mice were observed for up to 12 weeks.

Gene expression profiling using cDNA microarrays

The aRNAs from SP cells were labelled with Cy5 dye and those from MP cells were labelled with Cy3 dye. The dye-labelled aRNA samples were hybridised to a 29 138-spot Human Panorama Micro Array (Sigma-Aldrich) for 16 h at 45°C. The intensities of Cy5 and Cy3 fluorescence for every gene spot on the hybridised array were measured with a GenePix 4000B scanner (Axon Instrument, Austin, TX, USA), and were analysed with GenePix Pro 5.0 software (Axon Instrument). Global normalisation of the resultant data was carried out using Excel 2004 (Microsoft, Redmond, WA, USA). As a result, 24 730 genes were available for further analysis. The average expression ratio of Cy5 to Cy3 was obtained for each gene. A dye-swap experiment (labelling SP and MP cells with Cy3 and Cy5, respectively) was also performed. An average ratio of more than 2.0, reproducible in two experiments, was determined to indicate differential upregulation in SP cells.

RESULTS

Identification of SP cells in human bone sarcoma cell lines

To identify the CSCs of bone sarcomas, we tried to detect side population (SP) cells in bone and soft tissue sarcoma cell lines. As depicted in Figure 1A, the NY and MFH2003 cell lines included 0.38 and 5.28% SP cells, respectively. In each case, the percentage of SP cells was markedly diminished by treatment with verapamil, which is an inhibitor of the pumps responsible for the exclusion of Hoechst dye, indicating that this population truly represented SP cells. SP cells were hardly detected in the other cell lines (Figure 1B). Therefore, MFH2003, containing the highest proportion of SP cells, was selected and further analysed.

Isolation of SP cells and their repopulation as both SP and MP cells

After excluding dead cells and cellular debris on the basis of scatter signals and propidium iodide fluorescence, MFH2003 cells were sorted into SP and MP cells. As shown in Figure 2A, the G1 gate showed the SP cells that had negative/low patterns of staining with Hoechst 33342, and the G2 gate showed the main population cells that were positively stained with Hoechst 33342. To ascertain the

purity of sorted cells, the obtained SP (G1) cells and MP (G2) cells were re-analysed. The purity levels were 92.86 and 90.78% in the SP population and MP population, respectively. These results supported the specificity for further analysis using the resultant SP and MP cells.

To examine whether SP cells could generate both SP and MP cells, sorted SP and MP cells were further cultured *in vitro*. On day 14, the cells were re-stained with Hoechst 33342 and analysed by flow cytometry. We observed that SP cells re-populated both SP and MP cells. The ratio of SP cells to MP cells was still much higher than that before sorting. In contrast, SP cells were not detected in sorted MP cells.

Expression of *ABCG2* mRNA, which is a marker of SP cells, was increased in SP cells (Figure 2B). These results also supported the specificity for further characterisation of SP cells, especially with regard to their cancer-initiating ability.

Spherical colony formation

We next evaluated the ability of SP and MP cells to generate spherical colonies. A total of 2000 SP and MP cells were sorted and cultured immediately under conditions of serum starvation, providing an anchorage-independent environment. On day 14, SP cells showed spherical colony formation (Figure 3A). On the

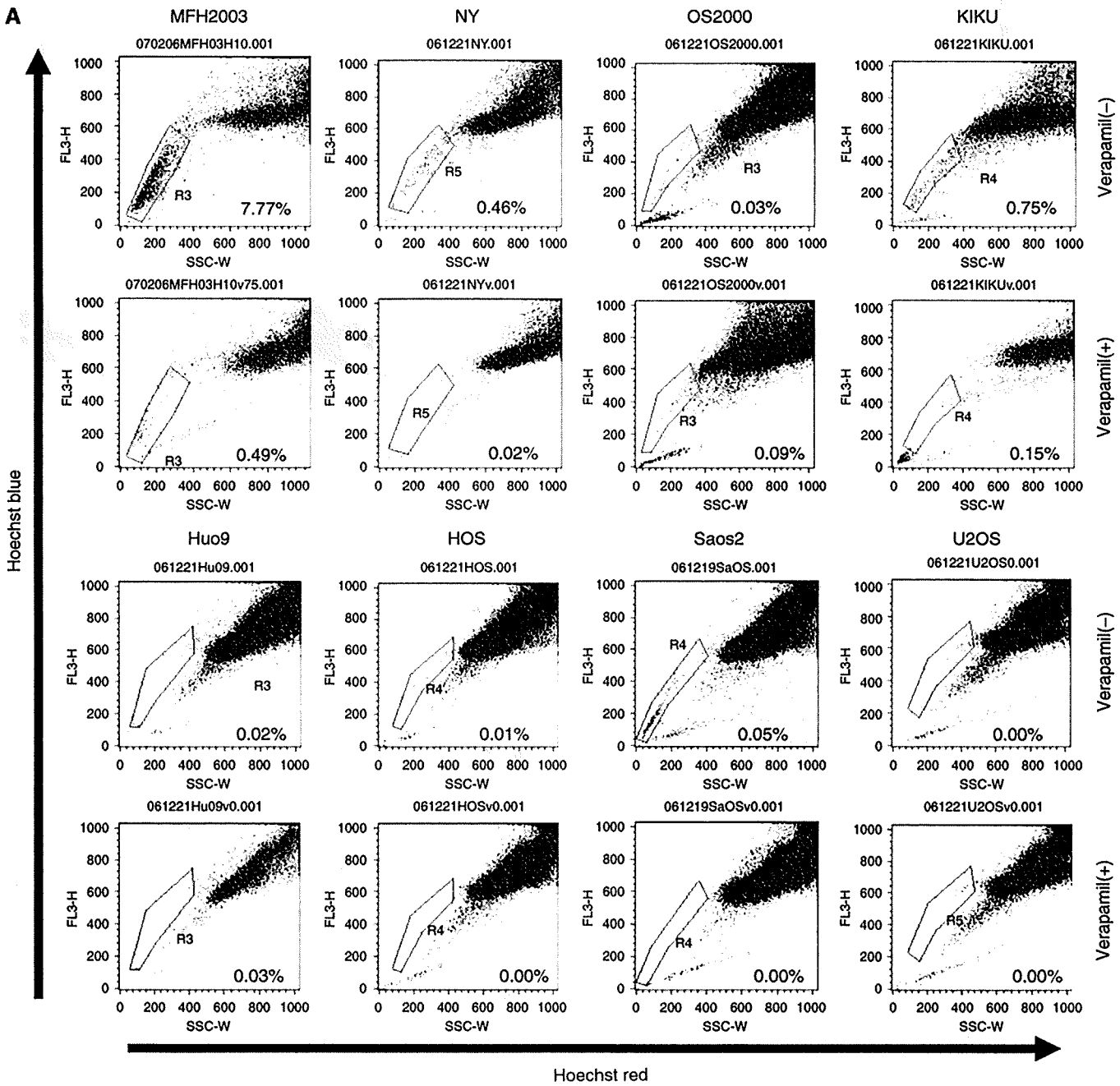

Figure 1 Detection of side population cells in bone sarcoma cell lines. (**A**) The populations of SP cells of seven osteosarcoma cell lines (NY, OS2000, KIKU, Huo9, HOS, Saos2 and U2OS) and of one bone MFH cell line (MFH2003), in the presence or absence of verapamil, are shown. SP cells are marked by black dotted lines to show the proportion of SP cells among total living cells. (**B**) The mean proportions of SP cells in cell lines. These results were reproducible in at least two independent experiments.

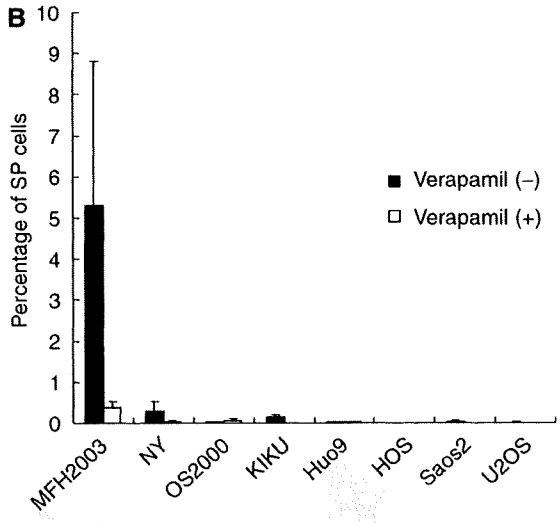

Figure 1 Continued.

other hand, as shown in Figure 3B, most MP cells died and the others formed a few small colonies. We removed spherical colonies from the suspension culture and attempted again to determine whether the cells could attach to a substratum. As shown in Figure 3C, cells were seen expanding from the sphere. In Figure 3D, the number of colonies is shown, indicating clearly that, among MFH2003 cells, SP, but not MP, cells had the potential for spherical colony formation.

Cancer-initiating ability of SP and MP cells *in vivo*

To address the issue of whether tumourigenic activity differed between SP and MP cells, $1 \times 10^2 - 1 \times 10^5$ SP and MP cells sorted from MFH2003 were injected into NOD/SCID mice (Figure 4A). To rule out the effects of the toxicity of Hoechst, we routinely performed (i) depletion of dead cells by PI staining and (ii) a viability check using trypan-blue staining after cell sorting. Almost all MP cells were viable as SP cells. Subcutaneous tumour formation was induced by the injection of 1×10^3 SP cells (Table 1). We also observed that 1×10^4 SP cells formed a larger tumour mass than did 1×10^3 SP cells (data not shown). In contrast, at least 1×10^5 MP cells were required to give rise to a tumour. Macroscopic and microscopic findings of a tumour derived from SP cells are shown in Figure 4A and B. These results supported the hypothesis that SP cells have a high cancer-initiating ability, similar to CSCs. At 8 weeks after xenotransplantation, the frequencies of SP and MP cells in a formed tumour derived from 1×10^4 SP cells were analysed *ex vivo*. SP cells were hardly detected in the tumour. Most SP cells re-populated into MP cells *in vivo* in 8 weeks (data not shown).

Identification of upregulated genes in SP cells

Finally, we performed gene expression profiling of SP cells using cDNA microarrays. As shown in Table 2, 23 genes were found to be upregulated in SP cells, compared with MP cells. Although the functions of upregulated genes varied, these results suggested that the factors connected to DNA transcription, transport of substrates, cell proliferation and apoptosis might have a role in the cancer-initiating ability of SP cells. In addition, the increased expression of *ABCG2* in SP cells confirmed the accuracy of the gene expression profiling analysis.

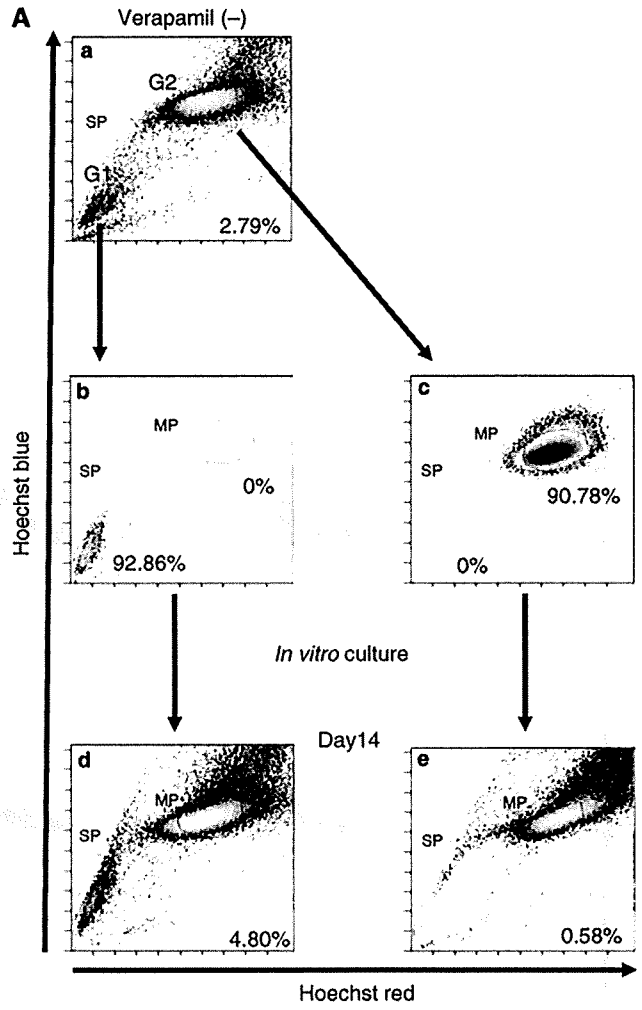

Figure 2 The re-population of SP cells into both SP and MP cells. (**A**) (**a**) The populations of SP cells and MP cells before cell sorting are shown. SP cells were gated as G1, and MP cells were gated as G2. (**b**, **c**) The proportions of SP cells among the total living cells are indicated. Isolated SP cells (**b**) and MP cells (**c**) after cell sorting. The proportions of SP and MP cells among the total living cells are indicated. (**d**, **e**) The populations of SP cells (**d**) and MP cells (**e**) after 2-week *in vitro* culture with medium containing 10% FBS are also shown. Experiments were repeated in triplicate with similar results. (**B**) The relative expression of ABCG2 was evaluated in SP cells and MP cells by real-time PCR.

DISCUSSION

In this study, we showed that (i) small SP populations existed in one osteosarcoma cell line and one bone MFH cell line; (ii) SP cells derived from MFH2003 could re-populate both SP and MP cells *in vitro*; (iii) SP cells could form spherical colonies and re-populate into SP and MP cells; (iv) SP cells had tumourigenesis in an *in vivo* xenograft model; and (v) factors regarding transcription, cell proliferation and apoptosis were upregulated in SP cells.

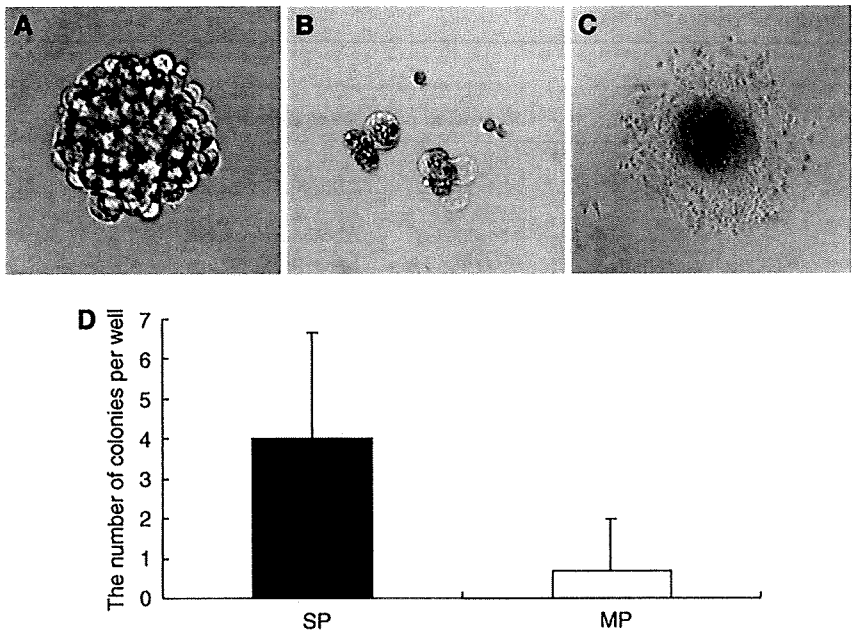

Figure 3 Tumourigenesis of SP and MP cells *in vitro*. (**A** and **B**) The features of spherical colonies derived from resultant SP cells (**A**) and MP cells (**B**) cultured without serum in an anchorage-independent manner for 2 weeks. (**C**) Spherical colony removed from the suspension culture and allowed to attach to a substratum. Adherent cells can be seen expanding from the sphere. (**D**) The numbers of resultant spherical colonies from SP cells and MP cells were counted. Data are representative of three independent experiments.

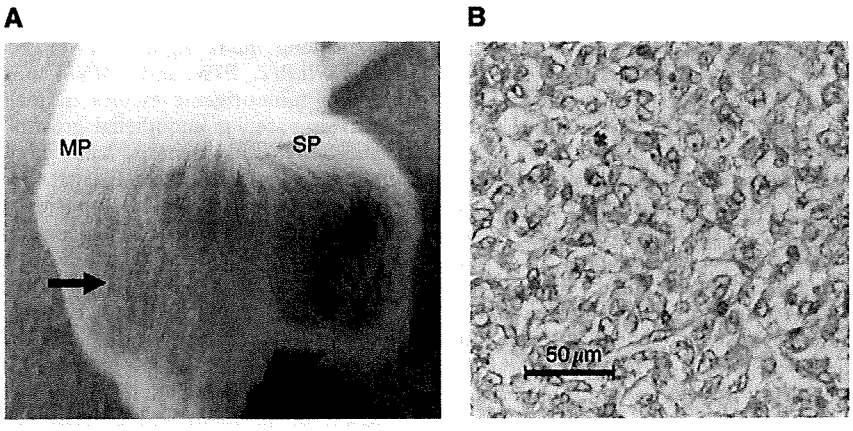

Figure 4 The features of xenotransplanted SP cells *in vivo*. (**A**) Macroscopic features of 1×10^3 each of SP and MP cells in an NOD/SCID mouse at 12 weeks after xenotransplantation. Black arrow indicates the site of injection of MP cells. (**B**) Histological findings of the xenotransplanted tumour derived from SP cells (1×10^4). Haematoxilin and eosin staining (original magnification: × 200) is shown.

Table 1 Tumorigenesis of SP and MP cells in NOD/SCID mice

	Cell number for injection			
	1×10^2	1×10^3	1×10^4	1×10^5
MFH2003				
SP cells	0/5	1/5	2/5	1/2
MP cells	0/5	0/5	0/5	1/2

SP and MP cells were isolated separately and injected into the backs of the subcutaneous space of NOD/SCID mice. Tumour formation was observed for 12 weeks after injection.

We observed proportions of SP cells of 0.31 and 5.28% in NY and MFH2003, respectively. The proportions of SP cells we observed were similar to those in most previous reports, with 2% noted in human breast cancer cell line MCF7, 0.4% in rat C6 glioma, 1.2% in human HeLa carcinoma (Kondo *et al*, 2004) and 4–37% in neuroblastoma cell lines (Hirschmann-Jax *et al*, 2004).

The SP cells were defined by the efflux of Hoechst 33342, a cell-permeable DNA-specific bisbenzimidazole dye, through an ABC transporter. Therefore, SP cells are considered to be resistant to multi-chemotherapeutic drugs and to confer malignant phenotypes to tumours (Dean *et al*, 2005). Hence, the characterisation of SP cells might be a useful tool for analysis of CSCs, especially when specific CSC surface markers are unknown.

We found that SP cells could re-populate both SP cells and MP cells *in vitro*. These results suggested that SP cells were capable of self-renewal and also generated MP cells by asymmetric division. This indicated that a tumour hierarchy might exist in bone MFH. Previous studies have also shown that SP cells can divide asymmetrically and display a capacity for self-renewal similar to

Table 2 List of genes upregulated in SP cells of MFH2003

Gene symbol	Gene name	Accession no.	Gene ontology	Expression ratio (SP/MP) Cy5/Cy3	Cy3/Cy5
ANKRD11	Ankyrin repeat domain 11	NM_013275	Electron transport	2.1	2.7
SLC2A4	Solute carrier family 2, member 4	NM_001042	Carbohydrate transport	2.2	2.5
KIAA1440	KIAA1440	AB037861	Unknown	2.2	3.3
SURF6	Surfeit 6	NM_006753	Ribosome biogenesis	2.3	2.8
VPF	Vascular permeability factor	M27281	Cell proliferation	3.0	3.5
C20orf14	Chromosome 20 open reading frame 14	NM_012469	RNA processing	2.1	3.6
PHLDA3	Pleckstrin homology-like domain, family A, member 3	NM_012396	Physiological processes	2.1	2.4
ZNF19	Zinc finger protein 19	NM_152907	Regulation of transcription	2.8	2.4
MCL1	Myeloid cell leukaemia sequence 1	NM_021960	Apoptosis	2.1	3.9
APOE	Apolipoprotein E	NM_000041	Lipid transport	2.1	3.8
NR4A2	Nuclear receptor subfamily 4, group A, member 2	NM_006186	Regulation of transcription	2.5	4.1
IRX3	Iroquois-related homeobox 3	BC023667	Regulation of transcription	3.3	2.9
GNB3	Guanine nucleotide-binding protein, β-polypeptide 3	NM_002075	G-protein coupled receptor protein signaling	2.1	5.0
NLRP12	NLR family, pyrin domain containing 12	NM_144687	Apoptosis	2.1	2.3
PTN	Pleiotrophin	NM_002825	Neurogenesis	2.0	2.6
ABCG2	ATP-binding cassette, sub-family G, member 2	NM_004827	Transport	2.2	2.9
APOL1	Apolipoprotein L	NM_145343	Lipid transport	2.2	2.6
MDFI	MyoD family inhibitor	NM_005586	Unknown	2.8	3.1
PRSS15	Protease, serine, 15	NM_004793	ATP-dependent proteolysis	2.1	2.5
MSX1	Msh homeo box homolog 1	NM_002448	Regulation of transcription	2.1	2.8
LDLR	Low density lipoprotein receptor	NM_000527	Cholesterol metabolism	2.1	3.1
LMNA	Lamin A/C	NM_170707	Cellular morphogenesis	2.1	2.9
MVK	Mevalonate kinase	BC016140	Cholesterol biosynthesis	2.2	2.1

Genes showing the ratio more than 2.0, which were reproducible in two experiments, were listed.

normal stem cells (Kondo *et al*, 2004; Singh *et al*, 2004). On the other hand, we also observed that most SP cells xenotransplanted in NOD/SCID mice re-populated into MP cells *in vivo*. SP cells might hardly be maintained *in vivo* for long time, that is, more than 8 weeks. In other words, the niche of the mouse model might not be adequate for the maintenance of SP cells derived from bone sarcoma cell lines, such as MFH2003.

The ability of SP cells to generate spherical colonies was higher than that of MP cells. This is consistent with previous studies (Patrawala *et al*, 2005; Mitsutake *et al*, 2007). We recognised that the difference was not a consequence of longer retention of Hoechst dye in MP cells, because MP cells were viable after staining with the dye, followed by sorting and maintenance in a culture medium with FBS. However, we cannot completely rule out the possibility that the difference was due to some effect of the Hoechst dye, which is potentially cytotoxic (Durand and Olive, 1982).

We could detect a higher tumourigenic potential of SP cells than of MP cells *in vivo* using a NOD/SCID xenograft model. In the field of bone and soft tissue sarcoma, only Wu *et al* (2007) succeeded in showing the *in vivo* cancer-initiating ability of CSCs derived from bone and soft tissue sarcomas, using SP cells isolated from fresh primary tumour tissues. The ability to consistently isolate MFH2003-derived SP cells allowed us to conduct SP cell-specific gene profiling. Moreover, it might become possible to identify CTL-defined CSC-specific tumour antigens for immunotherapy targeting CSCs. Thus far, we have been trying to identify CTL-defined tumour antigens by forward and reverse immunological approaches and have carried out antigenic peptide vaccination trials in bone and soft tissue sarcomas (Sato *et al*, 2002; Ida *et al*, 2004; Tsukahara *et al*, 2004, 2008a, b, 2009; Kawaguchi *et al*, 2005; Kimura *et al*, 2008). Currently, we are trying to establish autologous CTL clones recognising SP cells of MFH2003 from tumour-infiltrating lymphocytes.

Thus far, only Oct3/4, Nanog and CD133 were reported to be candidates for CSC-specific markers in bone and soft tissue sarcoma (Gibbs *et al*, 2005; Tirino *et al*, 2008). Therefore, the gene profile of SP cells might help to expand the possibility of an effective isolation of CSCs from bone and soft tissue sarcomas using these specific markers. In the current gene expression profiling, 23 genes with various functions were upregulated in SP cells. Among them, eight genes (*VPF*, *c20orf14*, *MCL1*, *NR4A2*, *IRX3*, *NRLP12*, *PTN* and *LMNA*) might be considered to be potential tumourigenic factors in malignancies. VPF, generally known as vascular endothelial growth factor, regulates vascular permeability, angiogenesis, cell migration and apoptosis in tumours (Nagy *et al*, 2008). C20orf14 is upregulated in lymphoma (Su *et al*, 2008) and HPV16/18-positive cervical cancer (Vazquez-Ortiz *et al*, 2007). MCL1 is a member of the B-cell lymphoma (BCL) family. MCL-1 negatively regulates pro-apoptotic factors (Bak and Bax) (Chen *et al*, 2007) and accelerates leukaemogenesis (Beverly and Varmus, 2009). NR4A2 belongs to the steroid nuclear hormone receptor superfamily and has a role in cell transformation in cervical cancer (Ke *et al*, 2004). IRX3 is epigenetically inactivated by methylation in CpG islands in brain tumours (Ordway *et al*, 2006) and prostate cancer (Morey *et al*, 2006). NLRP12, also known as RNO2/monarch-1, is reported to activate inflammation in humans (Ye *et al*, 2008). PTN is an angiogenic factor that stimulates tumour-associated vascular formation in many malignancies. (Perez-Pinera *et al*, 2008). LMNA is reported to encode lamin A, which is a putative colonic epithelial stem cell marker and is also a prognostic factor in colorectal cancer (Willis *et al*, 2008). On the other hand, four genes (*ANKRD11*, *PHLDA3*, *APOL1* and *MSX1*) are known as tumour-suppressor factors. ANKRD11 is a p53-interacting protein and activates the transcription of p53 in breast cancer. PHLDA3 is a positive regulator of Fas-dependent death signalling, related to cisplatin-mediated apoptosis (Kerley-Hamilton *et al*, 2005). APOL1 is classically thought to be involved in lipid transport and metabolism and has rarely been characterised with regard to cell survival. Although the structure of APOL1 is similar to that of the anti-apoptotic proteins of the Bcl-2 family (Vanhollebeke and Pays, 2006), it can induce autophagic cell death (Wan *et al*, 2008). MSX1, a homeobox gene important for embryonic neural crest development, can induce the inhibition of tumour-initiating ability in soft agar *in vitro*. Taken together, the gene expression profiling in SP cells derived from MFH2003 containing various tumour-proliferative and tumour-suppressive factors might indicate the complexity of maintaining the

characteristics of SP cells as tumour initiators. However, considering the characteristics of SP cells for cancer-initiating ability, the apoptosis-related molecules among these genes (MCL-1, ANKRD11, PHLDA3 and APOL1) might have roles in the proliferation of SP cells. Moreover, these molecules could be candidates for specific markers and, in addition, molecular therapeutic targets.

In conclusion, we identified SP cells in established human bone sarcoma cell lines. Moreover, we demonstrated that bone MFH-derived SP cells can re-populate both SP and MP cells and have cancer-initiating ability *in vitro* and *in vivo*. These findings supported the idea that bone sarcomas might contain a certain population of CSCs. Gene profiling of SP cells could serve to elucidate candidates for specific markers and therapeutic targets. Thus, further studies for the characterisation of CSCs in human bone and soft tissue sarcomas might contribute to the elucidation of the mechanisms of tumourigenesis and to the establishment of novel therapeutic strategies.

ACKNOWLEDGEMENTS

We thank Ms Keiko Miwa (Team for Cell Lineage Modulation, RIKEN Center for Developmental Biology, Kobe, Japan) for her technical support. This work was supported by Grants-in-Aid from the Ministry of Education, Culture, Sports, Science and Technology of Japan (Grant no. 16209013 to N Sato), from Practical Application Research from the Japan Science and Technology Agency (Grant no. H18-1 to T Torigoe), from the Ministry of Health, Labor and Welfare (Grant no. H17-Gann-Rinsyo-006 to T Wada) and from the Uehara Memorial Foundation (Grant no. H19-Kenkyu-Syorei to T Tsukahara).

REFERENCES

Al-Hajj M, Wicha MS, Benito-Hernandez A, Morrison SJ, Clarke MF (2003) Prospective identification of tumorigenic breast cancer cells. *Proc Natl Acad Sci USA* **100:** 3983–3988

Beverly LJ, Varmus HE (2009) MYC-induced myeloid leukemogenesis is accelerated by all six members of the antiapoptotic BCL family. *Oncogene* **28:** 1274–1279

Chen S, Dai Y, Harada H, Dent P, Grant S (2007) Mcl-1 down-regulation potentiates ABT-737 lethality by cooperatively inducing Bak activation and Bax translocation. *Cancer Res* **67:** 782–791

Collins AT, Berry PA, Hyde C, Stower MJ, Maitland NJ (2005) Prospective identification of tumorigenic prostate cancer stem cells. *Cancer Res* **65:** 10946–10951

Dean M, Fojo T, Bates S (2005) Tumour stem cells and drug resistance. *Nat Rev Cancer* **5:** 275–284

Durand RE, Olive PL (1982) Cytotoxicity, mutagenicity and DNA damage by Hoechst 33342. *J Histochem Cytochem* **30:** 111–116

Fletcher CDM, van den Berg E, Molenaar WM (2002) Pathology and genetics of tumors of soft tissue and bone. In: *World Health Organization Classification of Tumors*, Fletcher CDM, Unni KK, Mertens F (eds), pp 120–122. IARC press: Lyon

Gibbs CP, Kukekov VG, Reith JD, Tchigrinova O, Suslov ON, Scott EW, Ghivizzani SC, Ignatova TN, Steindler DA (2005) Stem-like cells in bone sarcomas: implications for tumorigenesis. *Neoplasia* **7:** 967–976

Goodell MA, Brose K, Paradis G, Conner AS, Mulligan RC (1996) Isolation and functional properties of murine hematopoietic stem cells that are replicating *in vivo*. *J Exp Med* **183:** 1797–1806

Haraguchi N, Utsunomiya T, Inoue H, Tanaka F, Mimori K, Barnard GF, Mori M (2006) Characterization of a side population of cancer cells from human gastrointestinal system. *Stem Cells* **24:** 506–513

Hermann PC, Huber SL, Herrler T, Aicher A, Ellwart JW, Guba M, Bruns CJ, Heeschen C (2007) Distinct populations of cancer stem cells determine tumor growth and metastatic activity in human pancreatic cancer. *Cell Stem Cell* **1:** 313–323

Hirschmann-Jax C, Foster AE, Wulf GG, Nuchtern JG, Jax TW, Gobel U, Goodell MA, Brenner MK (2004) A distinct 'side population' of cells with high drug efflux capacity in human tumor cells. *Proc Natl Acad Sci USA* **101:** 14228–14233

Ida K, Kawaguchi S, Sato Y, Tsukahara T, Nabeta Y, Sahara H, Ikeda H, Torigoe T, Ichimiya S, Kamiguchi K, Wada T, Nagoya S, Hiraga H, Kawai A, Ishii T, Araki N, Myoui A, Matsumoto S, Ozaki T, Yoshikawa H, Yamashita T, Sato N (2004) Crisscross CTL induction by SYT-SSX junction peptide and its HLA-A*2402 anchor substitute. *J Immunol* **173:** 1436–1443

Kawaguchi S, Wada T, Ida K, Sato Y, Nagoya S, Tsukahara T, Kimura S, Sahara H, Ikeda H, Shimozawa K, Asanuma H, Torigoe T, Hiraga H, Ishii T, Tatezaki SI, Sato N, Yamashita T (2005) Phase I vaccination trial of SYT-SSX junction peptide in patients with disseminated synovial sarcoma. *J Transl Med* **3:** 1

Ke N, Claassen G, Yu DH, Albers A, Fan W, Tan P, Grifman M, Hu X, Defife K, Nguy V, Meyhack B, Brachat A, Wong-Staal F, Li QX (2004) Nuclear hormone receptor NR4A2 is involved in cell transformation and apoptosis. *Cancer Res* **64:** 8208–8212

Kerley-Hamilton JS, Pike AM, Li N, DiRenzo J, Spinella MJ (2005) A p53-dominant transcriptional response to cisplatin in testicular germ cell tumor-derived human embryonal carcinoma. *Oncogene* **24:** 6090–6100

Kimura S, Kozakai Y, Kawaguchi S, Tsukahara T, Ida K, Murase M, Matsumura T, Kaya M, Torigoe T, Wada T, Sato N, Yamashita T (2008) Clonal T-cell response against autologous pleomorphic malignant fibrous histiocytoma antigen presented by retrieved HLA-A*0206. *J Orthop Res* **26:** 271–278

Kondo T, Setoguchi T, Taga T (2004) Persistence of a small subpopulation of cancer stem-like cells in the C6 glioma cell line. *Proc Natl Acad Sci USA* **101:** 781–786

Kruger JA, Kaplan CD, Luo Y, Zhou H, Markowitz D, Xiang R, Reisfeld RA (2006) Characterization of stem cell-like cancer cells in immune-competent mice. *Blood* **108:** 3906–3912

Lewis VO (2007) What's new in musculoskeletal oncology. *J Bone Joint Surg Am* **89:** 1399–1407

Li C, Heidt DG, Dalerba P, Burant CF, Zhang L, Adsay V, Wicha M, Clarke MF, Simeone DM (2007) Identification of pancreatic cancer stem cells. *Cancer Res* **67:** 1030–1037

Mitsutake N, Iwao A, Nagai K, Namba H, Ohtsuru A, Saenko V, Yamashita S (2007) Characterization of side population in thyroid cancer cell lines: cancer stem-like cells are enriched partly but not exclusively. *Endocrinology* **148:** 1797–1803

Morey SR, Smiraglia DJ, James SR, Yu J, Moser MT, Foster BA, Karpf AR (2006) DNA methylation pathway alterations in an autochthonous murine model of prostate cancer. *Cancer Res* **66:** 11659–11667

Nabeta Y, Kawaguchi S, Sahara H, Ikeda H, Hirohashi Y, Goroku T, Sato Y, Tsukahara T, Torigoe T, Wada T, Kaya M, Hiraga H, Isu K, Yamawaki S, Ishii S, Yamashita T, Sato N (2003) Recognition by cellular and humoral autologous immunity in a human osteosarcoma cell line. *J Orthop Sci* **8:** 554–559

Nagy JA, Benjamin L, Zeng H, Dvorak AM, Dvorak HF (2008) Vascular permeability, vascular hyperpermeability and angiogenesis. *Angiogenesis* **11:** 109–119

Ordway JM, Bedell JA, Citek RW, Nunberg A, Garrido A, Kendall R, Stevens JR, Cao D, Doerge RW, Korshunova Y, Holemon H, McPherson JD, Lakey N, Leon J, Martienssen RA, Jeddeloh JA (2006) Comprehensive DNA methylation profiling in a human cancer genome identifies novel epigenetic targets. *Carcinogenesis* **27:** 2409–2423

Patrawala L, Calhoun T, Schneider-Broussard R, Zhou J, Claypool K, Tang DG (2005) Side population is enriched in tumorigenic, stem-like cancer cells, whereas ABCG2+ and ABCG2- cancer cells are similarly tumorigenic. *Cancer Res* **65:** 6207–6219

Perez-Pinera P, Berenson JR, Deuel TF (2008) Pleiotrophin, a multi-functional angiogenic factor: mechanisms and pathways in normal and pathological angiogenesis. *Curr Opin Hematol* **15:** 210–214

Ricci-Vitiani L, Lombardi DG, Pilozzi E, Biffoni M, Todaro M, Peschle C, De Maria R (2007) Identification and expansion of human colon-cancer-initiating cells. *Nature* **445:** 111–115

Robinson SN, Seina SM, Gohr JC, Kuszynski CA, Sharp JG (2005) Evidence for a qualitative hierarchy within the Hoechst-33342 'side population' (SP) of murine bone marrow cells. *Bone Marrow Transplant* **35:** 807–818

Sato Y, Nabeta Y, Tsukahara T, Hirohashi Y, Syunsui R, Maeda A, Sahara H, Ikeda H, Torigoe T, Ichimiya S, Wada T, Yamashita T, Hiraga H, Kawai A, Ishii T, Araki N, Myoui A, Matsumoto S, Umeda T, Ishii S, Kawaguchi S, Sato N (2002) Detection and induction of CTLs specific for SYT-SSX-derived peptides in HLA-A24(+) patients with synovial sarcoma. *J Immunol* **169:** 1611–1618

Singh SK, Hawkins C, Clarke ID, Squire JA, Bayani J, Hide T, Henkelman RM, Cusimano MD, Dirks PB (2004) Identification of human brain tumour initiating cells. *Nature* **432:** 396–401

Su L, Chen D, Zhang J, Li X, Pan G, Bai X, Lu Y, Zhou J, Li S (2008) The expression and bioinformatic analysis of a novel gene C20orf14 associated with lymphoma. *J Huazhong Univ Sci Technolog Med Sci* **28:** 97–101

Szotek PP, Pieretti-Vanmarcke R, Masiakos PT, Dinulescu DM, Connolly D, Foster R, Dombkowski D, Preffer F, Maclaughlin DT, Donahoe PK (2006) Ovarian cancer side population defines cells with stem cell-like characteristics and Mullerian Inhibiting Substance responsiveness. *Proc Natl Acad Sci USA* **103:** 11154–11159

Takeuchi H, Kawaguchi S, Mizuno S, Kirita T, Takebayashi T, Shimozawa K, Torigoe T, Sato N, Yamashita T (2008) Gene expression profile of dorsal root ganglion in a lumbar radiculopathy model. *Spine* **33:** 2483–2488

Tirino V, Desiderio V, d'Aquino R, De Francesco F, Pirozzi G, Galderisi U, Cavaliere C, De Rosa A, Papaccio G (2008) Detection and characterization of CD133+ cancer stem cells in human solid tumours. *PLoS ONE* **3:** e3469

Tsukahara T, Kawaguchi S, Ida K, Kimura S, Tamura Y, Ikeda T, Torigoe T, Nagoya S, Wada T, Sato N, Yamashita T (2006) HLA-restricted specific tumor cytolysis by autologous T-lymphocytes infiltrating metastatic bone malignant fibrous histiocytoma of lymph node. *J Orthop Res* **24:** 94–101

Tsukahara T, Kawaguchi S, Torigoe T, Kimura S, Murase M, Ichimiya S, Wada T, Kaya M, Nagoya S, Ishii T, Tatezaki S, Yamashita T, Sato N (2008a) Prognostic impact and immunogenicity of a novel osteosarcoma antigen, papillomavirus binding factor, in patients with osteosarcoma. *Cancer Sci* **99:** 368–375

Tsukahara T, Kawaguchi S, Torigoe T, Murase M, Wada T, Kaya M, Nagoya S, Yamashita T, Sato N (2009) HLA-A*0201-restricted CTL epitope of a novel osteosarcoma antigen, papillomavirus binding factor. *J Transl Med* **7:** 44

Tsukahara T, Nabeta Y, Kawaguchi S, Ikeda H, Sato Y, Shimozawa K, Ida K, Asanuma H, Hirohashi Y, Torigoe T, Hiraga H, Nagoya S, Wada T, Yamashita T, Sato N (2004) Identification of human autologous cytotoxic T-lymphocyte-defined osteosarcoma gene that encodes a transcriptional regulator, papillomavirus binding factor. *Cancer Res* **64:** 5442–5448

Tsukahara T, Torigoe T, Tamura Y, Wada T, Kawaguchi S, Tsuruma T, Hirata K, Yamashita T, Sato N (2008b) Antigenic peptide vaccination: Provoking immune response and clinical benefit for cancer. *Curr Immunol Rev* **4:** 235–241

Vanhollebeke B, Pays E (2006) The function of apolipoproteins L. *Cell Mol Life Sci* **63:** 1937–1944

Vazquez-Ortiz G, Garcia JA, Ciudad CJ, Noe V, Penuelas S, Lopez-Romero R, Mendoza-Lorenzo P, Pina-Sanchez P, Salcedo M (2007) Differentially expressed genes between high-risk human papillomavirus types in human cervical cancer cells. *Int J Gynecol Cancer* **17:** 484–491

Visvader JE, Lindeman GJ (2008) Cancer stem cells in solid tumours: accumulating evidence and unresolved questions. *Nat Rev Cancer* **8:** 755–768

Wada T, Uede T, Ishii S, Matsuyama K, Yamawaki S, Kikuchi K (1988) Monoclonal antibodies that detect different antigenic determinants of the same human osteosarcoma-associated antigen. *Cancer Res* **48:** 2273–2279

Wan G, Zhaorigetu S, Liu Z, Kaini R, Jiang Z, Hu CA (2008) Apolipoprotein L1, a novel Bcl-2 homology domain 3-only lipid-binding protein, induces autophagic cell death. *J Biol Chem* **283:** 21540–21549

Warner JK, Wang JC, Hope KJ, Jin L, Dick JE (2004) Concepts of human leukemic development. *Oncogene* **23:** 7164–7177

Willis ND, Cox TR, Rahman-Casans SF, Smits K, Przyborski SA, van den Brandt P, van Engeland M, Weijenberg M, Wilson RG, de Bruine A, Hutchison CJ (2008) Lamin A/C is a risk biomarker in colorectal cancer. *PLoS ONE* **3:** e2988

Wu C, Wei Q, Utomo V, Nadesan P, Whetstone H, Kandel R, Wunder JS, Alman BA (2007) Side population cells isolated from mesenchymal neoplasms have tumor initiating potential. *Cancer Res* **67:** 8216–8222

Ye Z, Lich JD, Moore CB, Duncan JA, Williams KL, Ting JP (2008) ATP binding by monarch-1/NLRP12 is critical for its inhibitory function. *Mol Cell Biol* **28:** 1841–1850

Yin S, Li J, Hu C, Chen X, Yao M, Yan M, Jiang G, Ge C, Xie H, Wan D, Yang S, Zheng S, Gu J (2007) CD133 positive hepatocellular carcinoma cells possess high capacity for tumorigenicity. *Int J Cancer* **120:** 1444–1450

Zhou S, Morris JJ, Barnes Y, Lan L, Schuetz JD, Sorrentino BP (2002) Bcrp1 gene expression is required for normal numbers of side population stem cells in mice, and confers relative protection to mitoxantrone in hematopoietic cells *in vivo*. *Proc Natl Acad Sci USA* **99:** 12339–12344

Surg Today (2010) 40:347–356
DOI 10.1007/s00595-009-4082-x

SURGERY TODAY

Inhibition of Osteopontin Reduces Liver Metastasis of Human Pancreatic Cancer Xenografts Injected into the Spleen in a Mouse Model

KEISUKE OHNO[1], HIDEFUMI NISHIMORI[1], TAKAHIRO YASOSHIMA[4], KENJIRO KAMIGUCHI[2], FUMITAKE HATA[5], RIKA FUKUI[1], KOICHI OKUYA[1], YASUTOSHI KIMURA[1], RYUICHI DENNO[3], SHIGEYUKI KON[6], TOSHIMITSU UEDE[6], NORIYUKI SATO[2], and KOICHI HIRATA[1]

Departments of [1]Surgery and [2]Pathology, Sapporo Medical University School of Medicine, S1W17, Chuo-ku, Sapporo 060-8556, Japan
[3]Department of Nursing, Sapporo Medical University School of Health Sciences, Sapporo, Japan
[4]Laboratory of Sapporo Cancer and Integrative Medicine, Shinsapporo Keiaikai Hospital, Sapporo, Japan
[5]Doto Hospital, Sapporo, Japan
[6]Division of Molecular Immunology, Institute for Genetic Medicine, Hokkaido University, Sapporo, Japan

Abstract

Purpose. Pancreatic cancer is associated with the poorest prognosis of any digestive cancer due to the high incidence of liver metastasis. This study evaluated the possibility that osteopontin (OPN) RNA interference (RNAi) and anti-OPN antibody (Ab) could have anti-metastatic effects.

Methods. The differential gene expression was measured in a parental cell line, HPC-3, and an established highly liver metastatic cell line, HPC-3H4. This study investigated the effect of OPN RNAi and anti-OPN Ab on the metastatic ability of HPC-3H4 to the liver. An OPN RNAi-expressing vector was introduced into HPC-3H4 cells (HPC-3H4/miOPN), in which OPN production was reduced to the level of the parental HPC-3 cells. Finally, the ability of anti-OPN Ab to suppress liver metastasis was investigated.

Results. Osteopontin was upregulated 11.1-fold in HPC-3H4 in comparison to HPC-3. The metastatic rate of HPC-3H4/miOPN was significantly reduced to 25% in comparison to the 100% metastatic rate of HPC-3H4 and control HPC-3H4/miNeg cells ($P < 0.01$). The metastatic rate of the group given anti-OPN Ab was 50%.

Conclusion. OPN RNAi and anti-OPN Ab had remarkable inhibitory effects against liver metastasis by the pancreatic cancer cell line.

Key words Osteopontin · RNA interference · Pancreatic cancer · Liver metastasis

Introduction

Pancreatic cancer patients have an extremely poor prognosis because liver metastasis is commonly observed even after extensive curative surgery.[1] Some chemotherapeutic regimens, such as gemcitabine, prolong survival of patients with resectable pancreatic cancer,[2] but in almost all cases of pancreatic cancer with liver metastasis, chemotherapy, radiation, and extensive surgery are unable to achieve long-term survival. It is critically important for oncologists to introduce a novel therapeutic means to achieve better survival for patients suffering from pancreatic cancer.

A highly liver metastatic HPC-3H4 cell line was derived from the human pancreatic cancer cell, HPC-3, which shows a low metastatic potential. These lines were used to investigate the molecular mechanisms involved in the liver metastasis of pancreatic cancer. A cDNA microarray was used to analyze the genes differentially expressed in these two cell lines. The microarray analysis revealed a variety of differentially expressed genes. This revealed that osteopontin (OPN) was highly expressed in metastatic HPC-3H4 cells.

Osteopontin is a secreted glycophosphoprotein with cell-adhesive and migratory properties, which can bind to extracellular matrix proteins and signal transducing receptors.[3–5] The expression of OPN is correlated with the metastasis of some malignant neoplasms.[6,7]

The current study evaluated the possibility that OPN might play an important role in the development of pancreatic cancer metastasis, and that OPN RNAi and anti-OPN Ab could have an anti-metastatic effect.

Reprint requests to: H. Nishimori
Received: November 24, 2008 / Accepted: June 16, 2009

Materials and Methods

Cell Lines

The human pancreatic cancer line, HPC-3 (parental cell line), its established highly metastatic variant, HPC-3H4 (liver metastatic line), and established sublines (HPC-3H1, HPC-3H2, and HPC-3H3) were used in this study. The procedure for establishing such variants has been described previously.[8–14] HPC-3 was inoculated into the spleens (5×10^6 cells) of nude mice. The mice developed cachexia after several weeks. The mice were then killed and a few metastatic nodules were harvested aseptically. The cells were expanded in culture and designated HPC-3H1. Thereafter, each selection cycle was repeated four times to yield HPC-3H4. These cell lines were maintained in a humidified atmosphere of 95% air and 5% CO_2 at 37°C in RPMI 1640 medium (Asahi Techno Glass, Funabashi, Japan) supplemented with 10% fetal bovine serum (FBS; Gibco, Grand Island, NY, USA), 8 mg/l tylosin tartrate (Sigma-Aldrich, St. Louis, MO, USA), 50 units/ml penicillin, and 50 mg/ml streptomycin (Gibco). The cells were passaged and expanded by trypsinization of the cell monolayer and replating every 4–5 days. The culture medium was changed every 2–3 days.

Animals

Athymic female BALB/c nu/nu mice, 5–7 weeks old, weighing 20–22 g, and originating from the Central Institute for Experimental Animals (Kawasaki, Japan), were purchased from Clea Japan (Tokyo, Japan). The mice were maintained in a laminar airflow cabinet under specific pathogen-free conditions and also were provided with sterile food and water. All experiments were performed according to the institutional ethical guidelines on animal care.

cDNA Microarray Analysis

The differential gene expression was determined in the HPC-3 and HPC-3H4 cell lines. Poly(A)+ mRNA was extracted from cultured cell pellets using a FastTrack mRNA Isolation Kit (Invitrogen, Leek, the Netherlands) according to the manufacturer's instructions, and quantified spectrophotometrically. Double-stranded cDNA was synthesized from the purified poly(A)+ mRNA using the T7-(dt) 24 primer (5′-GGC CAG TGA ATT GTA AGT AAT ACG ACT CAC TAT AGG GAG GCG G-(dt) 24–3′) and a Superscript kit (Invitrogen, Carlsbad, CA, USA). Double-stranded cDNA was purified by phenol/chloroform extraction with phase-lock gels. Biotin-labeled antisense cRNA (target) in an in vitro transcription reaction (IVT) was produced using the ENZO BioArray RNA Transcript Kit (Affymetrix, Santa Clara, CA, USA). Thereafter, the IVT product (cRNA) was cleaned up using Qiagen RNeasy Columns (Qiagen, Hilden, Germany) according to the manufacturer's instructions. The cRNA was subsequently fragmented for target preparation. A hybridization cocktail was prepared using the Gene Chip Eukaryotic Hybridization Control Kit (Affymetrix). This cocktail was then hybridized on the Gene Chip Human Cancer G110 Array (Affymetrix) during a 16-h incubation in a 45°C oven. Immediately following hybridization, the hybridized probe array was subjected to an automated washing and staining protocol on the fluid station according to the Gene Chip Fluidics Station 400 User's Manual. Each probe array was scanned twice. The computer workstation automatically overlaid the twice-scanned images and averaged the intensities of each probe cell for the greatest assay sensitivity.

The data were analyzed using the Microarray Suite 4.0 software package (Affymetrix). The software calculated the average intensity of each probe array signal and then applied the selected array algorithm to determine the expression level for each gene. The average expression level of each gene in each cell line was calculated, as well as the ratio of the average expression level between the two cell lines.

Reverse Transcription–Polymerase Chain Reaction (RT-PCR) Analysis

Total RNA was isolated from each cultured cell pellet using the RNeasy Mini Kit (Qiagen) according to the manufacturer's instructions. First-strand cDNA was synthesized from 1 µg of total RNA using the Super Script Choice System for cDNA Synthesis (Invitrogen) in 19 µl of a reaction mixture according to the manufacturer's instructions. One microliter of synthesized first-strand cDNA was amplified by PCR in a final volume of 50 µl containing 5 µl of a 10× PCR buffer, 4 µl of 2.5 mM deoxynucleotide triphosphates (dNTP), 2 µl each of 10 µM forward and reverse primers, 0.5 µl of ExTaq polymerase (TaKaRa, Shiga, Japan) and 35.5 µl of water. The sequences of the primers for OPN and GAPDH used were 5′-TCC AAG TAA GTC CAA CGA AAG C-3′ (forward), 5′-GAC CTC AGT CCA TAA ACC ACA C-3′ (reverse) and 5′-GAG TCA ACG GAT TTG GTC GT-3′ (forward), 5′-TTA TTT TGG AGG GAT CTC G-3′ (reverse), respectively. PCR amplification of the cDNA was performed under the following conditions: 30 cycles, 15 s at 98°C, 2 s at 52°C, 30 s at 74°C. Before the first cycle, a denaturation step for 2 min at 98°C was included, and after 30 cycles the extension was prolonged for 7 min at 72°C.

Enzyme-Linked Immunosorbent Assay (ELISA) of OPN

The cells were cultured in 96-well plates at a cell density of 1×10^4 cells/well in an RPMI 1640 medium supplemented with 10% FCS for 24h, and, the next day, the culture medium was changed to serum-free RPMI 1640. After 2 days, the supernatants were collected, and the concentrations of OPN were measured using ELISA kits according to the manufacturer's instructions (IBL, Gunma, Japan). The data were normalized to cell number in the wells at the time of collection of conditioned medium with 1×10^4 cells.

Histological Treatment

To evaluate differences in histological features, 5×10^6 cultured cells were inoculated subcutaneously, and tumor specimens were fixed by the perfusion of 10% formaldehyde for 7–10 days. They were sectioned serially into 3-μm slices and stained with hematoxylin–eosin.

Immunohistochemical Study

Immunohistochemical staining was carried out using 4-μm-thick sections from formalin-fixed, paraffin-embedded tissues mounted on silane-coated glass slides. The tissues were deparaffinized in xylene and dehydrated through a graded alcohol series. The slides were heated in a 10mM citrate buffer by autoclaving for 10min at 120°C. Then, a monoclonal mouse antibody (1:100) against OPN (Anti-Human Osteopontin [10A16] Mouse IgG MoAb, IBL, Gunma, Japan) was applied overnight in a humid chamber at 4°C.

OPN-Expressing Vector Construction and Transfection

Human OPN cDNA was obtained by RT-PCR using total RNA from HPC-3H4 cells. The PCR oligonucleotides were 5′-CGG GAT CCA TGA GAA TTG CAG TGA TTT G-3′ (sense) and 5′-GGG AAG CTT GAC CTC AGA AGA TGC AC-3″ (antisense). The PCR product was digested with *Bam*HI and *Hin*dIII and cloned into pcDNA3.1/myc-His(–) A (Invitrogen) mammalian expression vector. The absence of undesired mutations in the construct was verified by sequencing.

Then, 2×10^4 HPC-3 cells were seeded at a 10-cm^2 surface area/plate with 2ml of an RPMI 1640 medium containing 10% FCS 24h before transfection. The transfection cocktail was made with 5μg of mixing plasmids (pcDNA3.1/OPN) and 15μl of Lipofectamine 2000 (Invitrogen) in 500μl of OptiMEM for 20min. The transfection was performed by adding the transfection cocktail to the culture medium. After 12h, the transfection cocktail was replaced with an RPMI 1640 medium containing 10% FCS. After 3 weeks of selection with 500μg/ml of G418, G418-resistant HPC-3 cells were cloned as HPC-3opn. The stable transfectant was maintained in a medium containing 100μg/ml of G418. HPC-3 cells transfected with an empty vector were cloned as HPC-3neg for a negative control.

OPN RNAi Design, Vector Construction, and Transfection

Nineteen-nucleotide (nt) DNA sequences targeting OPN were designed using the BLOCK-iT RNAi Designer at http://www.invitrogen.com/rnaidesigner. The sequences (5′-TGG CTA AAC CCT GAC CCA TCT-3′) corresponded to the sequence of human osteopontin mRNA (GenBank accession number: NM-000582). A 19-nt oligonucleotide 5′-GTC TCC ACG CAG TAC ATT T-3′, which had no significant homology to any known human mRNA in the databases, was used as a negative control. Synthetic sense and antisense oligonucleotides were used to create the template for generating RNA composed of two identical 19-nt sequence motifs in an inverted orientation separated by a 9-base-pair (bp) spacer to form a double-stranded hairpin of small interfering RNA. Two micrograms of each oligonucleotide was annealed by heating for 4min at 95°C and cooling for 10min to room temperature, and then ligated into 2μl of pcDNA 6.2-GW/EmGFP-miR, a linearized plasmid vector (containing the spectinomycin and Blasticidin resistance gene and the *Pol*II promoter; Invitrogen). These constructs were cloned in TOP10 chemically competent *Escherichia coli* cells according to the manufacturer's instructions (Invitrogen). The sequence of each insert was confirmed by automated sequencing. The two constructs were named pcDNA/miOPN as an OPN RNAi-expressing vector and pcDNA/miNeg as a negative control vector.

Next, 2×10^4 HPC-3H4 cells were seeded at 10-cm^2 surface area plates with 2ml of an RPMI 1640 medium containing 10% FCS 24h before transfection. The transfection cocktail was made by mixing 5μg of plasmids (pcDNA/miOPN or pcDNA/miNeg) and 15μl of Lipofectamine 2000 (Invitrogen) in 500μl of OptiMEM for 20min. The transfection was performed by adding the transfection cocktail to the culture medium. After 12h, the transfection cocktail was replaced with an RPMI 1640 medium containing 10% FCS. After 3 weeks of selection with 5μg/ml of Blasticidin, Blasticidin-resistant HPC-3H4 cells were cloned as HPC-3H4/miOPN and HPC-3H4/miNeg. The stable transformants

were maintained in a medium containing 5 μg/ml of Blasticidin.

Evaluation of Liver Metastatic Potential of Cell Lines

Cells (5×10^6) of each intended cell line were injected into the spleens of nude mice using a 27-gauge needle. The mice were killed approximately 4 weeks after the injection, and autopsies were performed thereafter. The ability of cells to produce liver metastasis in nude mice was evaluated microscopically.

Blocking Assay of Liver Metastasis in Vivo Using Anti-OPN Ab

First, 5×10^6 of HPC-3H4 cells suspended in 0.1 ml of PBS were injected into the spleens of nude mice. The mice were then randomly divided into two groups of ten animals each and given the following treatments: the OPN Ab group was injected intraperitoneally with an anti-OPN (M5) Ab,[15] and the control group was injected intraperitoneally with rabbit γ-globulin. Both treatments were administered on the day before and the day after inoculation at a dose of 450 μg dissolved in 1 ml of PBS. The mice were killed 4 weeks later, and the liver metastasis rate was calculated.

Statistical Analysis

Statistical differences were evaluated using the Mann–Whitney *U*-test and Fisher's exact test. *P* values of less than 0.05 were considered to be significant.

Results

Differential Gene Expression in a Liver Metastasis Cell Line

Table 1 shows the list of genes differentially expressed in HPC-3H4 in comparison to HPC-3. The ratio represents the expression value in a metastatic cell line, HPC-3H4, in comparison to that in the parental cell line, HPC-3. Nine upregulated genes and six downregulated genes were recognized to have over 5-fold expression differences in the ratio. Among differentially expressed genes, OPN was the most highly upregulated gene in HPC-3H4 in comparison to the HPC-3 line. The OPN mRNA expression level in HPC-3H4 was 11.1-fold that in HPC-3.

Relation of the Metastatic Rate and OPN Expression Among Cell Lines

The metastatic rates of the cell lines are presented in Fig. 1A. Four metastatic cell lines were established from the minimally/nonmetastatic HPC-3 parental cell line; HPC-3H4 with 100% metastatic ability, followed by HPC-3H3 with 90%, HPC-3H2 with 75%, and HPC-3H1 with less than 30%.

The expression of OPN transcripts was examined by nonquantitative RT-PCR (Fig. 1B) to investigate the role of OPN as a metastasis-related protein. The amplification of OPN in the highly metastatic cell lines seemed to be stepwise higher than that of the less metastatic cell lines. Amplified OPN fragments of the expected size (285 bp) were detected more strongly in HPC-3H4 than

Table 1. Differential gene expression in HPC-3H4 in comparison to that in HPC-3

Accession no.	Gene name	Intensity in HPC-3	Intensity in HPC-3H4	Ratio
Upregulated gene				
M28130	interleukin 8 (il8)	40.9	1284.3	31.0
M62402	insulin-like growth factor binding protein 6 (igfbp6)	−1.1	715.1	24.9
J04765	osteopontin	320.9	3111.6	11.1
U09937	urokinase-type plasminogen receptor	30.3	222.2	9.1
U04313	maspin	−9.4	241.3	9.0
M62403	insulin-like growth factor binding protein 4 (igfbp4)	42.9	326.4	8.4
U67988	guanylate kinase associated protein (gkap)	−11.2	145.4	6.4
M60314	bone morphogenetic protein 5 (bmp-5)	−0.5	153.2	6.4
L31584	G protein-coupled receptor (EBI 1)	9.0	159.1	6.0
Downregulated gene				
M22490	bone morphogenetic protein-2B (BMP-2B)	377.3	91.8	8.4
M14752	c-abl	133.5	4.5	7.2
U93867	RNA polymerase III subunit (RPC62)	65.7	−98.4	7.0
M35011	integrin beta-5	1156.6	169.7	6.8
U59423	Smad1	754.3	140.0	5.9
M90657	tumor antigen (L6)	3187.2	566.6	5.1

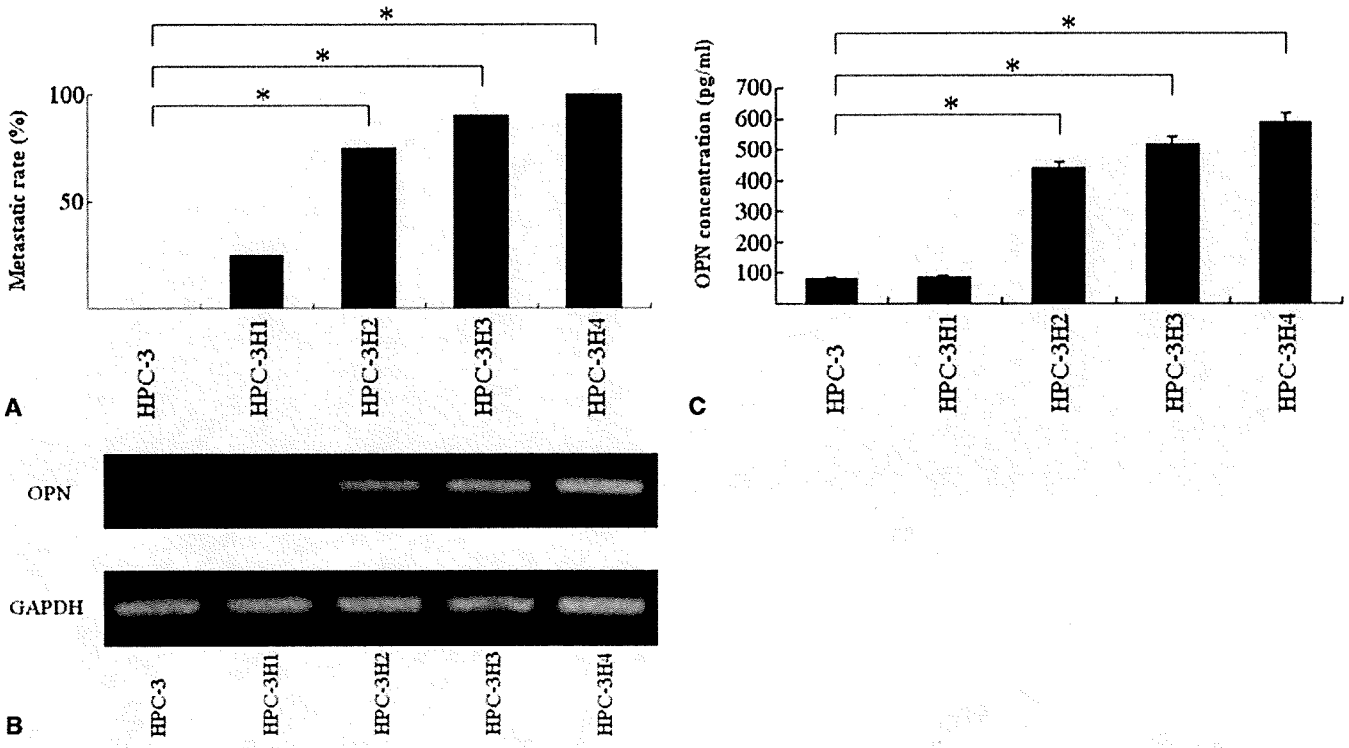

Fig. 1. A Metastatic rate of the established cell lines. The metastatic rate was higher in each metastatic subline than it was in each parental cell line. The numbers are the percentage values. *$P < 0.01$(Fisher's exact probability test) vs HPC-3. **B** Reverse transcription–polymerase chain reaction for the detection of osteopontin (*OPN*) mRNA. The amplification of OPN by the more metastatic cell line was stepwise higher than that of a lower metastatic cell line. Glyceraldehyde-3-phosphate dehydrogenase (*GAPDH*) is shown as a quantitative control. **C** Enzyme-linked immunosorbent assay of OPN production. OPN production by highly liver metastatic cell lines was significantly higher than that by the parental cell line. The results are expressed as mean ± SD. *$P < 0.01$, significantly different from HPC-3

in HPC-3. The identity of the amplified fragments was verified by sequencing.

The level of OPN protein expression by various cell lines was determined using an ELISA to correlate the degree of OPN expression with the metastatic potential. Figure 1C shows that the production of OPN by the highly metastatic cell lines was stepwise higher than that of less metastatic cell lines. The OPN levels of HPC-3, HPC-3H1, HPC-3H2, HPC-3H3, and HPC-3H4 were 85.3 ± 0.66, 87.0 ± 0.63, 439.7 ± 2.95, 517.6 ± 6.41, and 586.9 ± 9.89 pg/ml, respectively (mean ± SE). Osteopontin production by HPC-3H2, HPC-3H3, and HPC-3H4 were significantly higher than that by HPC-3 ($P < 0.01$).

Two representative cell lines, HPC-3 and HPC-3H4, were used in following experiments to further dissect the molecular role of OPN in liver metastasis. The histological features were initially examined. Two cell lines were injected into mice, and the tumor tissues that developed in vivo were stained with hematoxylin–eosin and immunohistochemically with the OPN antibody. There was no remarkable difference in the morphology between HPC-3 and HPC-3H4. The pathological findings corresponded to poorly differentiated adenocarcinoma, and the two cell lines had essentially the same appearance (Fig. 2). The immunohistochemical analysis showed a similar amount and pattern of OPN staining between the two cell lines (Fig. 2): OPN was mostly present in the cytoplasm of tumor cells.

Effect of Forced Alteration of the OPN Production Ability on Cell Lines

The metastatic ability was further analyzed by manipulating OPN expression by silencing the endogenous OPN gene or introducing an exogenous OPN gene. First, an HPC-3opn cell line was established, in which the exogenous OPN gene was introduced, and its negative control was the HPC-3neg cell line. Figure 3A shows that OPN production by HPC-3opn was 587.2 ± 2.80 pg/ml, which was similar to the level produced by the highly metastatic HPC-3H4 cells. In sharp contrast, both HPC-3neg and HPC-3 produced significantly lower amounts of OPN in comparison to HPC-3H4 cells. Consistent with the ELISA results, the amplifica-

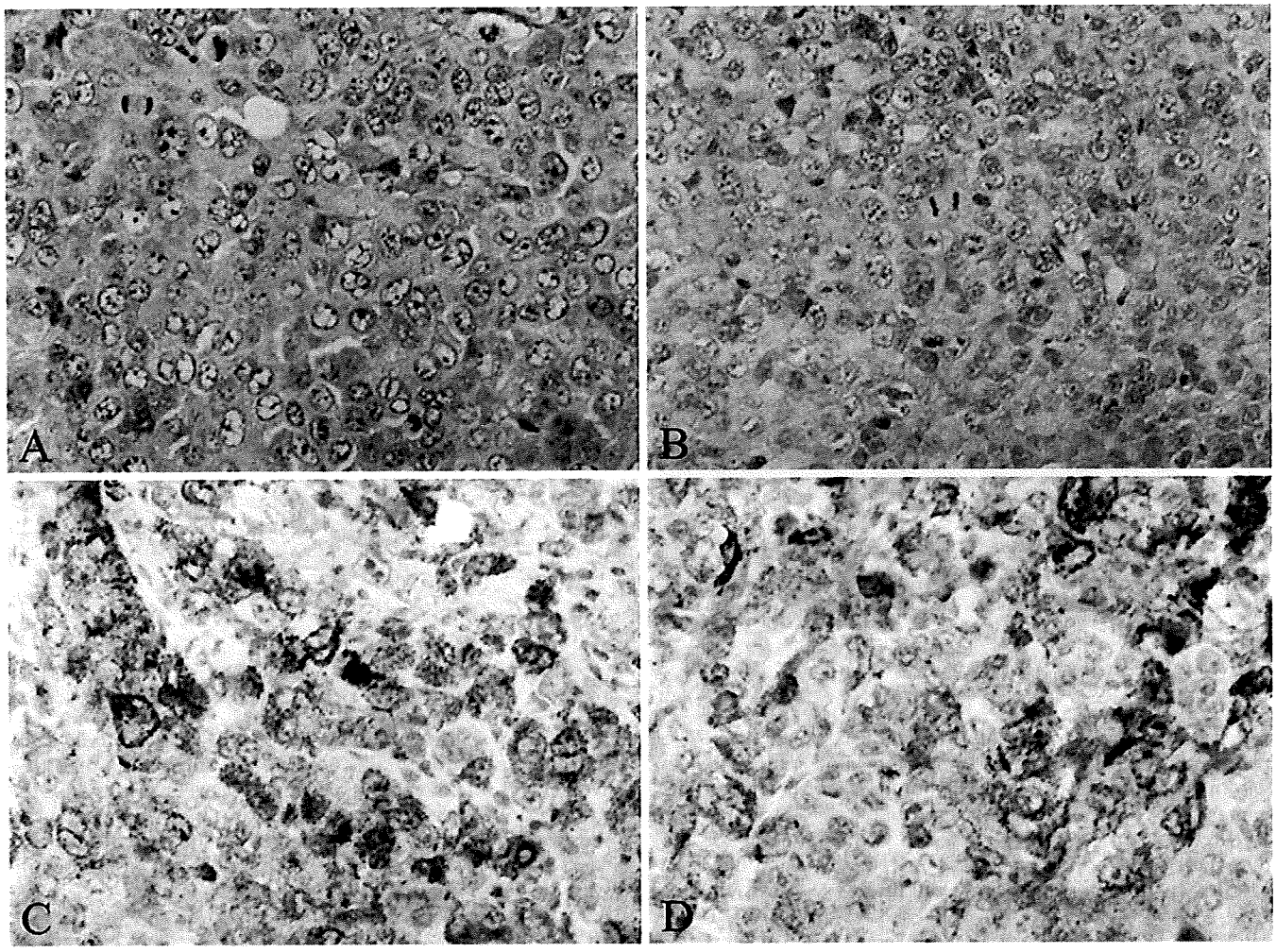

Fig. 2. Hematoxylin–eosin and immunohistochemical staining of tumors formed by cell lines. Histopathology of tumors showing poorly differentiated adenocarcinoma, with the same morphology of cancer growth. **A** HPC-3: parental tumor growing in a subcutaneous lesion, **B** HPC-3H4: a metastatic lesion growing in the liver. Immunohistochemical staining for OPN, with the same level of immunostaining intensity. OPN expression is localized in the cytoplasm of tumor cells and the extracellular matrix. **C** HPC-3: a parental tumor growing in a subcutaneous lesion. **D** HPC-3H4: metastatic lesion growing in the liver

tion of mRNA of OPN by HPC-3opn was at the same level as that by HPC-3H4, and was significantly stronger than that by HPC-3 and HPC-3neg (Fig. 3B).

Subsequently, the metastatic rate was evaluated using these cell lines. Unexpectedly, the metastatic rate of the HPC-3opn was 0% (0/10), which was the same as those of HPC-3 and HPC-3neg. Therefore, the introduction of exogenous OPN gene alone into low metastatic HPC-3 cells did not promote liver metastasis.

The following experiments attempted to inhibit the liver metastasis of highly metastatic HPC-3H4. An HPC-3H4/miOPN cell line was established, in which endogenous OPN expression was silenced by OPN RNAi and its negative control, HPC-3H4/miNeg cell line. Stable blocking of OPN by the RNAi-expressing vector was confirmed by verifying that the OPN production was at the same level in a transformant (HPC-3H4/miOPN) cultured for 1 week, a transformant (HPC-3H4/miOPN) cultured for 4 weeks, and a parental cell line (HPC-3) using an ELISA. Figure 3A shows that the OPN level in HPC-3H4/miOPN was 96.6 ± 0.68 pg/ml, which was significantly lower than that of HPC-3H4 and HPC-3H4/miNeg ($P < 0.01$) in ELISA. In addition, the amplification of OPN mRNA by HPC-3H4/miOPN was at the same level as that of low metastatic HPC-3 (Fig. 3B).

The metastatic rates of these established cell lines are presented in Fig. 3C. The metastatic rate of the HPC-3H4/miOPN was 25% (2/8), a significantly lower rate than those of HPC-3H4 and HPC-3H4/miNeg. Therefore, the silencing of the endogenous OPN expres-

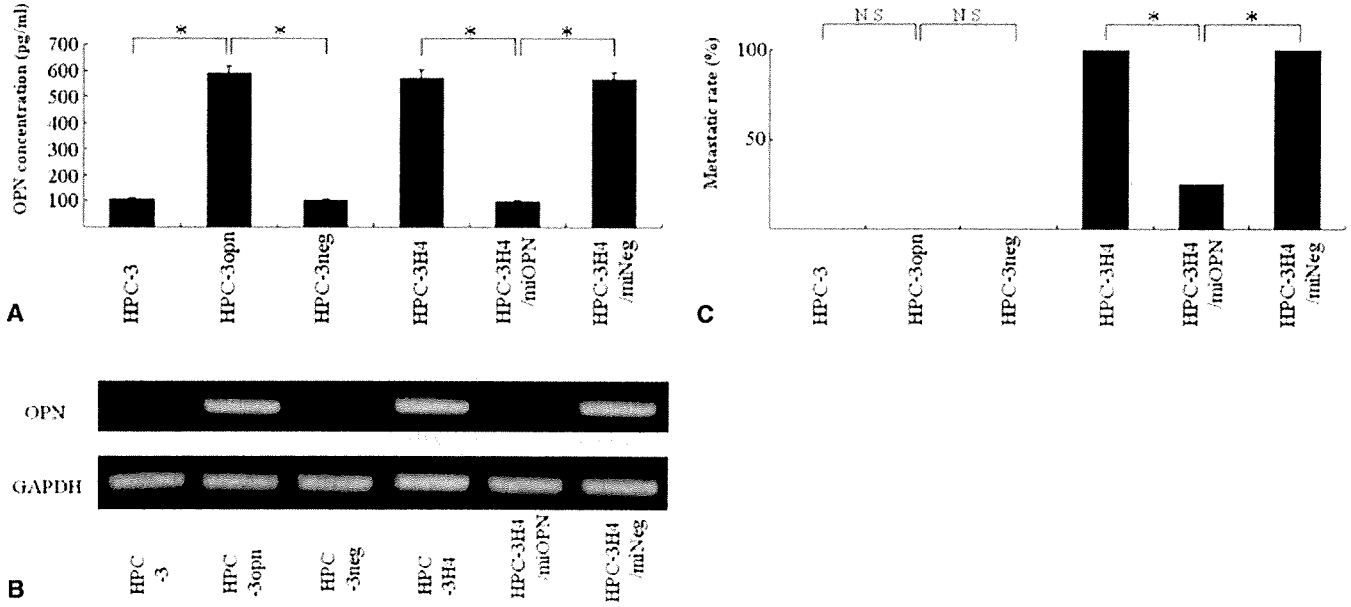

Fig. 3. **A** Enzyme-linked immunosorbent assay of OPN production. OPN production by HPC-3H4, HPC-3opn, and HPC-3H4/miR-neg was significantly higher than that by HPC-3, HPC-3neg, and HPC-3H4/miOPN. OPN production by HPC-3H4/miOPN was at the same level as that by HPC-3. The results are expressed as mean ± SD. $*P < 0.01$, significantly different from HPC-3opn and HPC-3H4/miOPN. **B** Reverse transcription–polymerase chain reaction for detection of OPN mRNA. An amplified fragment of the expected size (285 bp) was detected to a greater extent in HPC-3H4, HPC-3opn, and HPC-3H4/miNeg than in HPC-3, HPC-3neg, and HPC-3H4/miOPN. Glyceraldehyde-3-phosphate dehydrogenase (*GAPDH*) is shown as a quantitative control. **C** Metastatic rate of the cell lines. The metastatic rate of the OPN-forced expression cell line, HPC-3opn, is 0% (0/10), the same level as that of HPC-3. The metastatic rate of the OPN-suppressed expression subline, HPC-3H4/miOPN, is 25 (2/8). The OPN RNAi-expressing vector reduced the metastasis to the liver. The numbers are percentage values. $*P < 0.01$ (Fisher's exact probability test) vs HPC-3H4/miOPN

sion in HPC-3H4 cells significantly reduced the liver metastasis ($P < 0.01$).

Effect of Anti-OPN Ab on the Liver Metastasis of HPC-3H4 Cells

Finally, anti-OPN Ab or control Ab was administered into the peritoneal cavity of mice at 1 day before and after intrasplenic HPC-3H4 cell injection. The metastatic rate of the control group was 100% (10/10), while that of the metastatic rate of OPN Ab group was 50% (5/10; Fig. 4). All mice in the control group had multiple and bilateral liver metastatic nodules, while most of the mice in the OPN Ab group had only a single or several unilateral metastatic nodules. These results demonstrated that the anti-OPN Ab administration significantly reduced the liver metastatic rate of HPC-3H4, which is a highly metastatic cell line ($P < 0.01$).

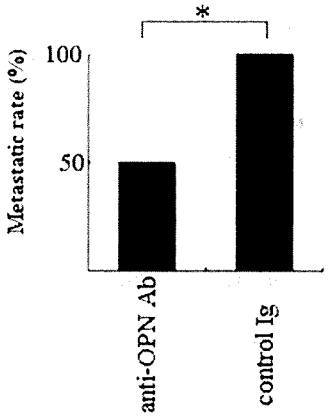

Fig. 4. Effect of anti-OPN antibody (*Ab*) on the liver metastasis of the HPC-3H4 cells in vivo. The metastatic rate of the control group (rabbit γ-globulin) was 100% (10/10), and all mice developed liver metastasis. On the other hand, the metastatic rate of the anti-OPN Ab group was 50% (5/10), and half of the mice developed liver metastasis. These results demonstrated that anti-OPN Ab administration reduced the liver metastatic rate of HPC-3H4. The numbers are percentage values. $*P < 0.01$ (Fisher's exact probability test) vs control

Discussion

Molecular-targeted agents, such as trastuzumab, which is effective against HER-2 overexpressed breast cancer,

have been applied in clinical settings and have yielded a high response rate. Molecular-targeted therapy is an ideal method with high specificity and fewer side effects for cancer therapy. Developments in molecular biology have resulted in the discovery of new genes or molecules in cancer patients, and allow oncologists to offer tailored treatments.

An exhaustive microarray analysis using two representative cell lines, an HPC-3H4 cell line with high metastatic potential to the liver and an HPC-3 cell line with a low metastatic potential, if any, to the liver was used to determine the metastasis-related genes of pancreatic cancer for molecular-targeted cancer therapy. The results indicated that the OPN gene was upregulated (11.1-fold) in the highly liver metastatic cell line, thus suggesting that OPN is one of the metastasis-related genes in pancreatic cancer.

Osteopontin is a 44-kDa secreted arginine-glycine-aspartate (RGD) containing glycophosphoprotein, and is a member of the small integrin-binding N-linked glycoprotein (SIBLING) family with cell-adhesive and migratory properties, normally produced by osteoblasts, arterial smooth muscle cells, various epithelia, activated T cells, and macrophages.[3] Osteopontin is able to bind to signal-transducing receptors (integrin receptors, CD44v).[4,5] It functions, either in the soluble condition like a cytokine or chemokine, or as an immobilized cell adhesive matrix protein. Osteopontin has been implicated in several distinct steps during complicated processes of tumorigenesis and cancer metastasis. Osteopontin is involved in the proliferation and progression of cancer,[16] the promotion of invasion,[17] binding with matrix metalloproteinases, apoptosis,[18] and the enhancement of the metastatic ability of cancer cells.[6] In clinical studies, augmented OPN expression has been associated with decreased survival in cancer patients,[19] increased metastatic potential,[7] and advanced disease staging.[20] Importantly, OPN is a tumor marker or a prognostic factor in a variety of malignancies including breast cancer,[21] lung cancer,[22] ovarian cancer,[23] prostate cancer,[16] liver cancer,[24] and colon cancer.[20] The down-regulation of OPN mRNA expression is associated with the suppression of the metastatic potential of breast cancer or hepatocellular carcinoma.[25–27]

The current study clearly demonstrated that the degree of OPN production was correlated with the metastatic rate of HPC-3 derived cell lines. The results also support the notion that serum OPN has a diagnostic potential as a biomarker for pancreatic diseases, as previously reported.[28,29]

An HPC-3opn cell line containing an exogenous OPN gene was established to further correlate the association between metastasis and OPN expression. This cell line produced OPN at a similar level to HPC-3H4. As shown in Fig. 1, there was a correlation between the potential of liver metastasis and OPN production. However, the metastatic rate of HPC-3opn was 0% at 4, 8, and 16 weeks. In fact, the development of cancer metastasis might not be regulated with only a single metastasis-related gene, and complicated genetic alterations and steps might be needed for metastasis formation.[30] It should be noted that OPN-induced increase in cell invasiveness is urokinase (urokinase-type plasminogen activator; uPA)-dependent.[31] Therefore, OPN-induced cell invasion and migration are inhibited by a uPA inhibitor and Abs against uPA or uPA receptor.[31] the current microarray data (Table 1) provided supporting data in which the uPA receptor was significantly upregulated in highly metastatic HPC-3H4, but not in low metastatic HPC-3. It is possible that transfection of both OPN and uPA allowed HPC-3 cells to be highly metastatic. This should be tested in future studies.

In contrast, HPC-3H4/miOPN was established, in which the production of OPN was suppressed by transfection of an OPN RNAi-expressing vector. Osteopontin production in HPC-3H4/miOPN declined to the same level as that in HPC-3. The metastatic rate of HPC-3H4/miOPN was 25% at 4 weeks, and the metastatic pattern was mild, with a lesser number of metastatic nodules. Therefore, the suppression of liver metastasis was achieved after the silencing of OPN expression by RNAi.

Moreover, the inhibitory effect of liver metastasis was assessed using the anti-OPN Ab. The dose of the anti-OPN Ab was based on the results of a previous report.[10] The metastatic rate in the control group was 100% at 4 weeks. On the other hand, in the group given the anti-OPN antibody, 50% of the mice showed complete inhibition of liver metastasis.

Therefore, these results might lead to the development of novel antimetastatic agents against pancreatic cancer metastasis. Previous reports[32,33] suggested that OPN was associated with the adhesion between tumor cells and the vascular endothelium, and that OPN was associated with such adhesion in various metastatic steps. Binding of OPN to cell-surface integrins might influence the ability of the tumor cells to bind to extracellular matrix components and thereby affect their ability to invade surrounding tissue. This might explain why the suppression and blockage of OPN clearly inhibited liver metastasis, as shown in the current study, although further study is needed to clarify the role of OPN in the development of pancreatic cancer metastasis.

Conclusion

The present study suggests that the expression of the OPN gene plays an important role in pancreatic cancer

progression, and is the first to demonstrate that the inhibition of OPN is effective in reducing the liver metastasis of pancreatic cancer in vivo. In addition, these results suggest that the OPN RNAi and anti-OPN Ab could be used for novel therapeutic strategies for the inhibition of pancreatic cancer metastasis. However, this study represents observations made in just one cell line. Further studies to assess the clinical impact of the OPN-Ab in pancreatic cancer metastasis are therefore needed in other cell lines before any definitive conclusions can be made.

References

1. Yokoyama Y, Nimura Y, Nagino M. Advances in the treatment of pancreatic cancer: Limitations of surgery and evaluation of new therapeutic strategies. Surg Today 2009;39:466–75.
2. Oettle H, Post S, Neuhaus P, Gellert K, Langrehr J, Ridwelski K, et al. Adjuvant chemotherapy with gemcitabine vs observation in patients undergoing curative-intent resection of pancreatic cancer. JAMA 2007;297:267–77.
3. O'Brien ER, Garvin MR, Stewart DK, Hinohara T, Simpson JB, Schwartz SM, et al. Osteopontin is synthesized by macrophage, smooth muscle, and endothelial cells in primary and restenotic human coronary atherosclerotic plaques. Artesioscler Thromb 1994;14:1648–56.
4. Weber GF, Ashkar S, Glimcher MJ, Cantor H. Receptor-ligand interaction between CD44 and osteopontin(Eta-1). Science 1996; 271:509–12.
5. Bayless KJ, Davis GE. Identification of dual α4β1 integrin binding sites within a 38 amino acid domain in the N-terminal thrombin fragment of human osteopontin. J Biol Chem 2001;276:13483–9.
6. Oates AJ, Barraclough R, Rudland PS. The identification of osteopontin as a metastasis-related gene product in a rodent mammary tumour model. Oncogene 1996;13:97–104.
7. Hotte SJ, Winquist EW, Stitt L, Wilson SM, Chambers AF. Plasma osteopontin: associations with survival and metastasis to bone in men with hormone-refractory prostate carcinoma. Cancer 2002;95:506–12.
8. Nishimori H, Yasoshima T, Denno R, Shishido T, Hata F, Honma T, et al. A new peritoneal dissemination model established from human pancreatic cancer cell line. Pancreas 2001; 22:348–56.
9. Shishido T, Yasoshima T, Hirata K, Denno R, Mukaiya M, Ura H, et al. Establishment and characterization of human pancreatic carcinoma lines with a high metastatic potential in the liver of nude mice. Surg Today 1999;29:519–25.
10. Nishimori H, Yasoshima T, Hata F, Denno R, Yanai Y, Nomura H, et al. A novel nude mouse model of liver metastasis and peritoneal dissemination from the same human pancreatic cancer line. Pancreas 2002;24:242–50.
11. Nomura H, Nishimori H, Yasoshima T, Hata F, Sogahata K, Tanaka H, et al. A new experimental mouse model of peritoneal dissemination of human gastric cancer cells: analysis of the mechanism of peritoneal dissemination using cDNA macroarrays. Jpn J Cancer Res 2001;92:748–54.
12. Nomura H, Nishimori H, Yasoshima T, Hata F, Tanaka H, Nakajima F, et al. A new liver metastatic and peritoneal dissemination model established from the same human pancreatic cancer cell line: analysis using cDNA macroarray. Clin Exp Metastasis 2002;19:391–99.
13. Yamaguchi K, Ura H, Yasoshima T, Shishido T, Denno R, Hirata K. Establishment and characterization of a human gastric carcinoma cell line that is highly metastatic to lymph nodes. J Exp Clin Cancer Res 2000;19:113–20.
14. Ohno K, Hata F, Nishimori H, Yasoshima T, Yanai Y, Sogahata K, et al. Metastatic-associated biological properties and differential gene expression profiles in established highly liver and peritoneal metastatic cell lines of human pancreatic cancer. J Exp Clin Cancer Res 2003;22:623–31.
15. Yamamoto N, Sakai F, Kon S, Morimoto J, Kimura C, Yamazaki H, et al. Essential role of the cryptic epitope SLAYGLR within osteopontin in a murine model of rheumatoid arthritis. J Clin Invest 2003;112:181–8.
16. Thalmann GN, Sikes RA, Devoll RE, Kiefer JA, Markwalder R, Klima I, et al. Osteopontin: possible role in prostate cancer progression. Clin Cancer Res 1999;5:2271–7.
17. Wu Y, Denhardt DT, Rittling SR. Osteopontin is required for full expression of the transformed phenotype by the ras oncogene. Br J Cancer 2000;83:156–63.
18. Ophascharoensuk V, Giachelli CM, Gordon K, Hughes J, Pichler R, Brown P, et al. Obstructive uropathy in the mouse: role of osteopontin in interstitial fibrosis and apoptosis. Kidney Int 1999;56:571–80.
19. Rudland PS, Platt-Higgins A, El-Tanani M, De Silva Rudland S, Barraclough R, Winstanley JH, et al. Prognostic significance of the metastasis-associated protein osteopontin in human breast cancer. Cancer Res 2002;62:3417–27.
20. Agrawal D, Chen T, Irby R, Quackenbush J, Chambers AF, Szabo M, et al. Osteopontin identified as lead marker of colon cancer progression, using pooled sample expression profiling. J Natl Cancer Inst 2002;94:513–21.
21. Kim YW, Park YK, Lee J, Ko SW, Yang MH. Expression of osteopontin and osteonectin in breast cancer. J Korean Med Sci 1998;13:652–7.
22. Shijubo N, Uede T, Kon S, Maeda M, Segawa T, Imada A, et al. Vascular Endothelial Growth Factor and Osteopontin in Stage I Lung Adenocarcinoma. Am J Respir Crit Care Med 1999;160: 1269–73.
23. Kim JH, Skates SJ, Uede T, Wong KK, Schorge JO, Feltmate CM, et al. Osteopontin as a potential diagnostic biomarker for ovarian cancer. JAMA 2002;287:1671–9.
24. Ye QH, Qin LX, Forgues M, He P, Kim JW, Peng AC, et al. Predicting hepatitis B virus-positive metastatic hepatocellular carcinomas using gene expression profiling and supervised machine learning. Nat Med 2003;9:416–23.
25. Mi Z, Guo H, Russell MB, Liu Y, Sullenger BA, Kuo PC. RNA aptamer blockade of osteopontin inhibits growth and metastasis of MDA-MB231 breast cancer cells. Mol Ther 2008;17:153–161.
26. Sun BS, Dong QZ, Ye QH, Sun HJ, Jia HL, Zhu XQ, et al. Lentiviral-mediated miRNA against osteopontin suppresses tumor growth and metastasis of human hepatocellular carcinoma. Hepatology 2008;48:1834–42.
27. Zhao J, Dong L, Lu B, Wu G, Xu D, Chen J, et al. Down-regulation of osteopontin suppresses growth and metastasis of hepatocellular carcinoma via induction of apoptosis. Gastroenterology 2008;135:956–68.
28. Koopmann J, Fedarko NS, Jain A, Maitra A, Iacobuzio-Donahue C, Rahman A, et al. Evaluation of osteopontin as biomarker for pancreatic adenocarcinoma. Cancer Epidemiol Biomarkers Prev 2004;13:487–91.
29. Kolb A, Kleeff J, Guweidhi A, Esposito I, Giese NA, Adwan H, et al. Osteopontin influences the invasiveness of pancreatic cancer cells and is increased in neoplastic and inflammatory conditions. Cancer Biol Ther 2005;4:740–6.
30. Hanahan D, Weinberg RA. The hallmarks of cancer. Cell 2000;100:57–70.
31. Tuck AB, Hota C, Chambers AF. Osteopontin (OPN)-induced increase in human mammary epithelial cell invasiveness is urokinase (uPA)-dependent. Breast Cancer Res Threat 2001;70: 197–204.

32. Behrend EI, Craig AM, Wilson SM, Denhardt DT, Chambers AF. Reduced malignancy of ras-transformed NIH 3T3 cells expressing antisense osteopontin RNA. Cancer Res 1994;54: 832–7.

33. Miyauchi A, Alvarez J, Greenfield EM, Teti A, Grano M, Colucci S, et al. Recognition of Osteopontin and related peptide by anαvβ3 integrin stimulates immediate cell signals in osteoclasts. J Biol Chem 1991;266:20369–74.

Immune response against tumor antigens expressed on human cancer stem-like cells/tumor-initiating cells

Cancer stem-like cells (CSCs)/tumor-initiating cells (TICs) are a small population of cancer cells that have the properties of tumor-initiating ability, self-renewal and differentiation. These properties suggest that CSCs/TICs are essential for tumor maintenance, recurrence and distant metastasis. Thus, elimination of CSCs/TICs is essential to cure malignant diseases. However, there are several studies reporting that CSCs/TICs are more resistant to standard cancer therapies, including chemotherapy and radiotherapy, than non-CSC/TIC populations. How then, can we eliminate CSCs/TICs? Immunotherapy might be the possible answer. In recent analysis, innate immunity (natural killer cells and γδT cells) and also adaptive immunity (cytotoxic T lymphocyte-based cellular immunity and antibody-based humoral immunity) can recognize CSCs/TICs *in vitro* efficiently. Furthermore, CSC/TIC-specific monoclonal antibody therapies are also efficient *in vivo*. In this article, we describe the potency, possibilities and problems of CSC/TIC-targeting immunotherapy.

KEYWORDS: antigenic peptide cancer stem cell CTL immunotherapy monoclonal antibody tumor antigen

Yoshihiko Hirohashi[1], Toshihiko Torigoe[2], Satoko Inoda[1], Akari Takahashi[1], Rena Morita[1], Satoshi Nishizawa[1], Yasuaki Tamura[1], Hiromu Suzuki[2], Minoru Toyota[2] & Noriyuki Sato[†1]

[†]Author for correspondence:
[1]Department of Pathology, Sapporo Medical University School of Medicine, South-1 West-17, chuo-ku, Sapporo 060-8556, Japan
Tel.: +81 116 138 374
Fax: +81 116 432 310
nsatou@sapmed.ac.jp
[2]Department of Biochemistry, Sapporo Medical University School of Medicine, Sapporo, Japan

Antigen-specific immune responses based on $CD8^+$ cytotoxic T lymphocytes (CTLs) and antibodies are essential for tumor rejection in the immune reaction against cancer cells. At the end of the 20th Century, cancer immunity research moved into a new stage when the first human tumor-associated antigen (TAA) recognized by CTLs was identified by van der Bruggen *et al.* [1]. With the identification of TAAs, cancer immunotherapy moved into a new era of specific cancer immunity, and cancer immunotherapy based on TAAs is becoming a reality [2]. CTLs recognize 9- to 14-mer antigenic peptides that are derived from endogenously expressed proteins digested by several proteases, including proteasomes and endoplasmic reticulum-associated aminopeptidase associated with antigen processing (ERAAP). Antibodies are other major players in specific immunity. Antibody-based immunotherapy can target only the cell surface proteins or secreted proteins such as $p185^{HER2/neu}$ for breast carcinoma, CD20 for B-cell lymphoma and VEGF for colorectal carcinoma. These CTL-based and antibody-based cancer immunotherapies are being developed in several ways and have already been launched all over the world. Of course, for cancer immunotherapy, various problems remain to be overcome. These problems include several immune escapse mechanisms such as antigen loss, HLA loss, immune suppressive cytokines, immunosuppressive cells such as regulatory T cells, regulatory dendritic cells and myeloid-derived suppressor cells, and immunosuppressive molecules such as indoleamine 2,3-dioxygenase (IDO).

Research into cancer stem-like cells (CSCs)/tumor-initiating cells (TICs) have made huge progress recently. CSCs/TICs are defined as the small population of cancer cells, which have the abilities of tumor initiation, self-renewal and differentiation. When we focus on clinical aspects of CSCs/TICs they have huge impact, since CSCs/TICs are resistant to standard therapeutic modalities, including chemotherapy and radiotherapy in various mechanisms. Thus, CSCs/TICs are thought to cause disease recurrence post-therapy, making the disease untreatable. Therefore, efficient CSC/TIC targeting therapy is needed to cure cancer. In this article, we focus on cancer immunotherapy as one of the representative way to treat CSCs/TICs.

Cancer stem cell hypothesis & isolation of cancer stem cell/tumor initiating cell population

It is well known that tumors are composed of morphologicaly and functionaly heterogeneous cells, and it has long been suspected that cancers may contain a small stem cell-like population (cancer stem cell hypothesis). Lapidot *et al.* had first given an explanation to this hypothesis [3]. They showed that human acute myeloid leukemia (AML) contained a small percentage of

future medicine part of fsg

cells (0.1–1%) capable of transferring human AML into immunodeficient mice. The resulting leukemia recomposed morphological and immunophenotypic heterogeneity resembling the original disease. The leukemia-initiating cells/leukemia stem cells (LSCs) could be isolated by cell surface markers ($CD34^+CD38^-$). More importantly, the nonleukemia stem cell phenotype ($CD34^+CD38^+$) did not engraft mice. This study clearly showed that LSCs were located at the top of the hierarchical organization of AML and harbor the ability to differentiate into matured differentiated leukemic cells, and only LSCs can initiate the disease. In subsequent studies, CSCs/TICs were isolated from several solid tumors by various methods. The use of cell surface markers (e.g., $CD34^+CD38^-$, $CD44^+CD24^-$ and CD133), side population (SP) and ALDEFLUOR® (StemCell Technologies Inc., USA) assay are representative methods for isolating CSCs/TICs today, as described in the following sections (FIGURE 1).

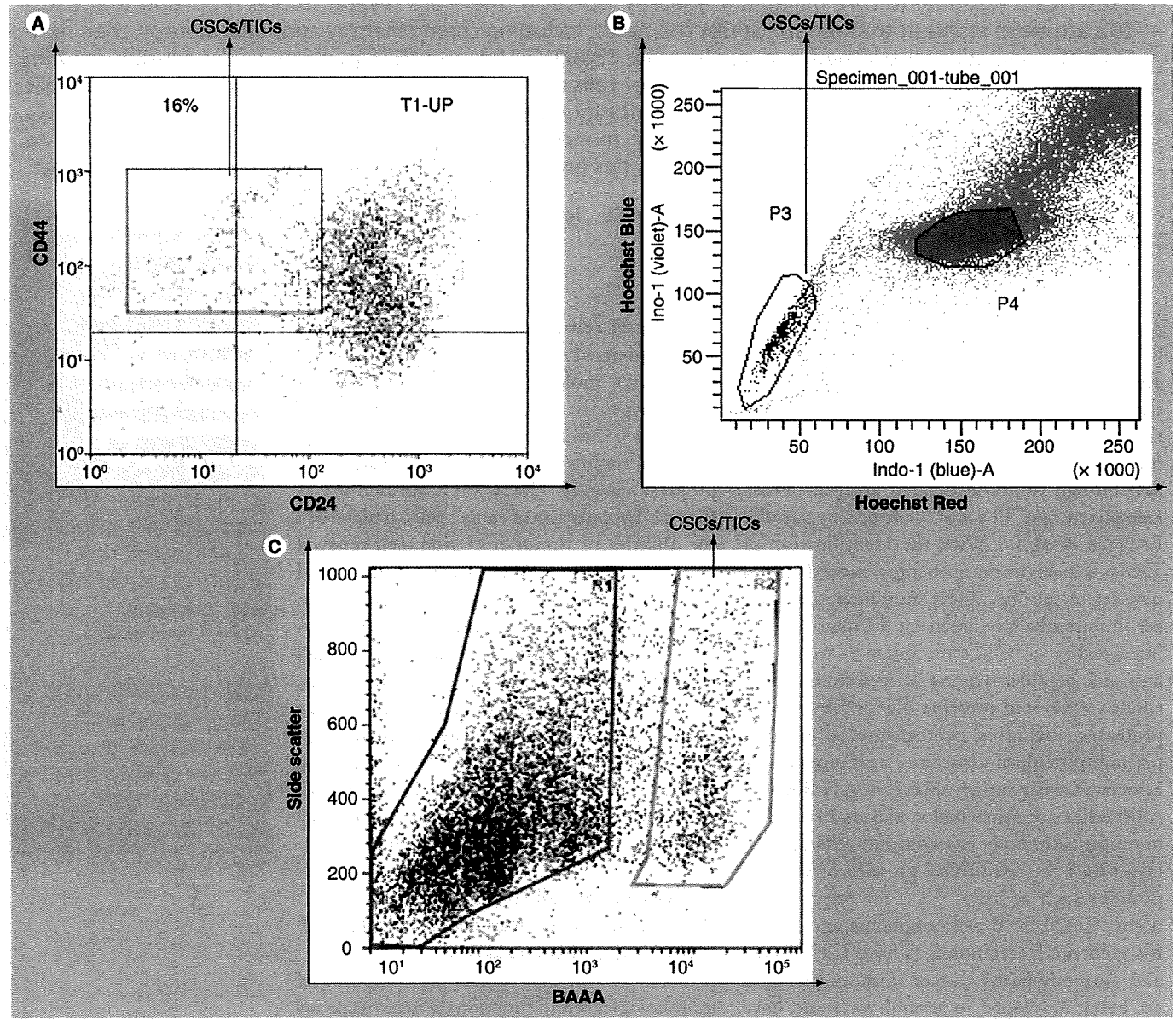

Figure 1. Isolation of cancer stem-like cells/tumor-initiating cells population. (A) Isolation of CSCs/TICs by cell surface markers. Breast cancer CSCs/TICs can be isolated as $CD44^+CD24^{-/low}$ population. **(B)** Isolation of CSCs/TICs as side population (SP) cells. CSCs/TICs express ABCG2 protein, which export Hoechst33342 dye, thus, CSCs/TICs can be isolated as low-stained populations. **(C)** Isolation of CSCs/TICs as ALDEFLUOR®-positive cells. CSCs/TICs express ALDH1 enzyme, thus, CSCs/TICs can be isolated as BAAA fluorescence.
CSC/TIC: Cancer stem-like cell/tumor-initiating cell.
(A) is reproduced with permission from [5]. **(C)** is reproduced from [31].

However, sometimes CSC/TIC-like populations isolated by those methods do not show the cancer stem cell properties, so it is essential to qualify the CSC/TIC-like populations as enriched cancer stem cell populations by methods such as xenotransplantation.

Cell surface markers

The first major method of isolating CSCs/TICs is the use of cell surface markers, such as LSCs, as previously described. Cell-surface markers for solid tumors have also been identified. Previously, we isolated CD44 as one of the cell-surface antigens that is related to the transformation of rat fibloblast cells with H-Ras oncogene [4]. Conversely, CD44 is not expressed in the normal fibroblast counterpart. This suggests that CD44 might be one of the highly tumorigenic cell (tumor-initiating cell) markers. We also found that CD44 can be the target of NK cells, raising the possibility that tumor-initiating cells may be eliminated by NK cells. In a later study, CD44 was identified as a marker for solid tumor CSCs/TICs by Al-Hajj *et al* [5]. They demonstrated that $CD44^+CD24^{-/low}$ breast cancer cells have high tumor-initiating ability in non-obese diabetic (NOD/SCID) mice. This population, representing 11–35% of cells in primary breast tumors, gave rise to tumors that recapitulated the morphologic and immunophenotypic features of the original tumor. In addition, these same cells could be sorted from the primary grafts and serially transplanted, demonstrating their self-renewal capability. The same group demonstrated that $CD44^+CD24^{-/low}$ expressed 186 genes (termed as invasive gene signature) compared with normal breast epithelia. Invasive gene signature positive group showed high risk of both metastasis-free survival and overall survival. This supports the idea that CSC/TIC populations have great impact *in vivo* [6]. In the following works, several other solid tumor CSCs/TICs have been identified in colon [7], pancreatic [8], prostate [9], head and neck squamous cell carcinomas [10], gastric carcinoma [11] and bladder carcinoma [12] using CD44 as a marker of CSCs/TICs. CD90 could be used for isolating CSCs/TICs of hepatocellular carcinoma [13]. The neural stem cell marker CD133 has been used for isolating CSCs/TICs of glioblastoma, medulloblastoma [14,15], colon cancer [16,17], pancreas cancer [18] and lung cancer [19]. However, Shmelkov *et al.* reported controversial data concerning CD133. They found that both $CD133^+$ and $CD133^-$ colon cancer cells could be xenotransplanted serially, and $CD133^-$ colon cancer cells made more aggressive tumors than $CD133^+$ colon cancer cells [20]. One ATP-binding cassette (ABC)-transporter gene product, ABCB5, was isolated as a melanoma-initiating cell marker [21].

Side population

The second method is using SP cells, that can be isolated by the effulux of $Hoechst_{33342}$ dye [22]. CSCs/TICs express various types of ABC transporters, including those encoded by the multidrug-resistant (*MDR*) gene 1, the multidrug-resistance-like protein (MRP) and ABCG2, which contribute to drug resistance in many cancers by pumping the drugs out of the cells. Importantly, some of these transporters are also expressed by small populations that have stem cell phenotypes. ABCG2 pumps out the fluorescent dye $Hoechst_{33342}$, which enables identification of the unlabeled SP cells as CSCs/TICs. Kondo *et al.* reported that mouse C6 glioma SP cells have multidifferentiation ability and high tumorigenicity [23]. Several reports demonstrated that GI tract cancer [24], hepatocellular carcinoma [25], thyroid cancer [26], nasopharyngeal cancer [27], lung cancer [28] and bone sarcoma [29] SP cells were enriched with CSC/TIC populations, suggesting that SP cells could be used for isolating CSCs/TICs. Conversely, Burkert *et al.* reported that GI tract SP cells were not enriched with CSCs/TICs [30]. Thus, in some cells, the SP cell phenotype might not correlate with the CSCs/TICs phenotype.

ALDEFLUOR® assay: ALDH1 expression

The third method is the ALDEFLUOR assay, which is based on the enzymatic activity of aldehyde dehydrogenase (ALDH)1. Ginestier *et al.* reported that breast cancer CSCs/TICs could be isolated as ALDH1 enzymatic positive cells [31]. The $ALDH1^+$ breast cancer cells were isolated by ALDEFLUOR assay using a cell sorter. Only the $ALDH1^+$ breast cancer cells were xenotransplantable. $ALDH1^+$ and $CD44^+/CD24^{-/lin-}$ breast cancer cells showed more efficient tumor-initiating ability than $ALDH1^+$ breast cancer cells. On the other hand, $ALDH1^-$ and $CD44^+/CD24^{-/lin-}$ breast cancer cells did not show any tumor-initiating ability. These data suggest that ALDH1 is more essential than $CD44^+/CD24^{-/lin-}$ in tumor-initiating ability. More importantly, $ALDH1^+$ breast cancer cases show the basaloid phenotypes related